Six strategies to produce application tailored nanoscale multilayer structured PVD coatings by conventional and High Power Impulse Magnetron Sputtering (HIPIMS)

HOVSEPIAN, Papken <http://orcid.org/0000-0002-1047-0407> and EHIASARIAN, Arutiun <http://orcid.org/0000-0001-6080-3946>

Published version

HOVSEPIAN, Papken and EHIASARIAN, Arutiun (2019). Six strategies to produce application tailored nanoscale multilayer structured PVD coatings by conventional and High Power Impulse Magnetron Sputtering (HIPIMS). Thin Solid Films, p. 137409.

Six Strategies to Produce Application Tailored Nanoscale Multilayer Structured PVD Coatings by Conventional and High Power Impulse Magnetron Sputtering (HIPIMS)

Author: 1
Prof. Papken Ehiasarian Hovsepian
Sheffield Hallam University, City Campus, Howard Street, Sheffield - S1 1WB, UK.
E-mail: P.Hovsepian@shu.ac.uk
Telephone: 0114 225 3644

Author: 2
Prof. Arutiun Papken Ehiasarian
Sheffield Hallam University, City Campus, Howard Street, Sheffield - S1 1WB, UK.

Abstract

The application field of functional coatings produced by Physical Vapor Deposition, (PVD) is ever expanding. Consequently the demand for novel materials exhibiting extraordinary properties is growing intensively. The paper summarises the experience and the expertise gained at Sheffield Hallam University in UK through work dedicated to the development of such advanced materials spanning more than two decades. It discusses six strategies to produce PVD coatings where the main three steps followed in any coating development process namely material selection, structure selection and finally coating deposition method consideration have been application informed. All described coatings however, utilise nanoscale multilayer structure and have been deposited by Direct Current Unbalanced Magnetron Sputtering (DCMS) or the novel High Power Impulse Magnetron Sputtering (HIPIMS) techniques.

Key words: Nanostructured coatings; High Power Impulse Magnetron Sputtering; boundary lubrication; orthopaedic implants; turbine blades; oxidation and corrosion resistance tribology.

1 Introduction

The quest for novel materials exhibiting extraordinary properties has generated a vast number of exciting ideas for their fabrication. Nanolayered materials, "superlattices" were discovered early in 1925 by Johanson and Linde as periodic structures of layers of two (or more) materials, [1] and used in many applications such as X-ray mirrors, magnetic recording media, and the semiconductor industry. In 1970 James Koehler at the University of Illinois in the US, proposed the idea that a man- made material can be created, which could match or exceed the hardness of diamond. It was suggested that this could be achieved by a layered structure of two materials with significant difference in their shear moduli provided that the thickness of the individual layers is in the nanometre range and more precisely when the bilayer repeat

period, Δ is in a narrow range of Δ≈3-10 nm, [2]. Various theories and models have been proposed to explain the material properties enhancement effects observed with such structures. For example the material strengthening was explained by the Hall-Petch effect, [3] the elastic moduli enhancement was related to the "Super modulus effect", [4] whereas the coherency stress, which develops due to the difference in the lattice constants that hinders dislocation motion was explained by the "Coherency stress effect", [5]. Xi Chu and Scott Barnett's introduced a model describing hardness- superlattice period relation where the hardness enhancement was explained by dislocation blocking by layer interfaces, [6]. Perhaps one of the most comprehensive papers describing the properties of these artificially grown structures was published in 1987 by the Linkoping University group in Sweden on TiN/VN, [7] reporting on the exciting possibility to produce a "superhard" (H > 40 GPa) thin films by magnetron sputtering . The first application of AlN/TiN superlattice coatings deposited by Cathodic Arc Evaporation on cutting tools was reported in 1996 by Sumitomo of Japan, [8]. Whereas results from a systematic research leading to the development of the first superlattice coating family of application tailored coatings produced by the Arc Bond Sputtering (ABS) technique, [9] were reported by the Surface Engineering Research group at Sheffield Hallam University in UK in 2000, [10]. A detailed description of the structure, properties and applications of these coatings is given in Ref. [11].

It is a requirement of the modern age that improvements in performance should not necessarily lead to a proportionate increase in cost. It is therefore imperative for the coating process that the deposition technique itself does not enhance the cost, whereas the influence of the material costs cannot be avoided. Substantial effort has been employed in the development of PVD deposition processes, which allow the manufacturing of coatings on the same price level as conventional binary nitrides such as TiN. Magnetron sputtering has been

found to be the most appropriate deposition technology, [12] although attempts have also been made to deposit such coatings by cathodic arc evaporation [8].

To achieve a reasonably economical process, complicated installations, including shielding and shuttering that reduce the deposition rate need to be avoided. In addition, reactive gas control should not be too complicated, in order to avoid high equipment costs. To satisfy these demanding requirements, the deposition processes used for the developments reported in the current paper have been carried out on an industrial size multiple target HTC-1000-4 PVD coater manufactured by Hauzer Techno Coating Europe, Venlo, The Netherlands enabled with High Power Impulse Magnetron Sputtering, (HIPIMS) technology at Sheffield Hallam University, UK.

For the successful application of the superlattice structured coatings however, it is essential to understand the consequences of using superhard materials. The superhardness is always related to high residual stress therefore coatings with hardness in the range H = 30-35 GPa were found to be usable in the largest range of industrial applications. Furthermore, with superhard materials, guaranteeing high coating adhesion is of paramount importance. Highest adhesion is achieved by ion bombardment, (etching) of the surface prior to the coating deposition using metal ions generated by Arc discharge. This approach has been well understood with early TiN arc deposited coatings, [13] and later transferred to the Arc Bond Sputtering technique. Surface pre-treatment utilising arc discharge guarantees shallow metal ion implantation, preserves crystallinity on small areas of the substrate which promotes local epitaxial coating growth and therefore enhanced adhesion, [14]. A disadvantage of this technology is however, the contamination of the bombarded surface with droplet macroparticles emitted by the cathode spots of the arc discharge, [15]. Due to the poor metallurgical interaction, (bonding) of the droplets with the substrate material they effectively reduce the adhesion-contributing surface area of the interface thus reducing the adhesion

overall. Additionally the droplet macroparticles act as points for development of growth defects, which heavily compromise coating density, [16]. Utilisation of filtered arc eliminates the droplet macroparticles but produces a sub-surface zone of high defect density at the interface. In comparison when Argon glow discharge is used for surface pre-treatment the crystallinity of the interface is completely lost. In this case, several nanometers thick amorphised zone is observed, as shown in Figure 1a, which compromises the adhesion strength.

These disadvantages are completely eliminated when a HIPIMS discharge is employed to generate the metal ions used for the surface pre-treatment, [17]. It is well documented that HIPIMS can produce highly ionised plasma in which the prevalent ions are metal (60%) rather than gas, where the metal-to-gas ion ratio is a linear function of the plasma density (peak current density) and the sputtering yield of the material. The metal ions can be multiply-ionised with the maximum charge state determined by the occupancy of the outer shells of the atom (the group in the periodic table), which, for transition group metals, are the d- and s- -shells. For example for Vanadium with an electron configuration of [Ar] $3d^3 4s^2$ the maximum state of significant abundance is 5+ at typical HIPIMS conditions [18]. At low gas pressures the discharge can be maintained at a high ionisation degree whilst the mean free path remains similar to the cathode-to-substrate distance and long enough to allow practically collisionless transport of ions to the substrate. This is important in order to avoid charge exchange reactions with Ar atoms which efficiently eliminate all metal ion states whose ionisation potential is greater than that of the first ionisation potential of the working gas; for metals in Ar this means all states above 2+ or even 1+.

The interface was found to be free of contaminations and amorphous phases such as native oxides. The high content of metal ions in the bombarding flux modifies the interface to include a 5-10 nm deep metal implantation zone that promotes a strong bond between the

substrate and the subsequently deposited coating. At the same time the metal implantation is by substitution and preserves the crystallinity of the implanted zone. In contrast, gas ion cleaning results in inert atom implantation as interstitials which severely deform the lattice structure. The clean interface and metal implantation zone provides a fully crystalline microstructure at the coating- substrate interface, (Figure 1b) and promote the alignment of the coating growth orientation to the crystal orientation of the substrate in two (epitaxial) or one directions (axiotaxial growth). The local crystallographic orientation is observed on large areas of the substrate of several micrometers across. The interface microstructure engineering by HIPIMS for enhanced adhesion is presented in details elsewhere [19]. Following this approach it was realised that the overall coatings deposited after HIPIMS pre-treatment exhibit superior adhesion in comparison to pre-treatments in Ar glow discharge and Cathodic Arc discharge.

The highly ionised plasma of HIPIMS provides conditions for effective ion bombardment of the growth surface hence increased ad-atom mobility on the surface of growing films. The first report on the properties of ceramic CrN film deposited by HIPIMS showing that the coatings exhibit a fully dense microstructure and a smooth surface, was published in 2004, [20]. Further research on TiN films confirmed these results. HRTEM revealed that TiN coatings with no intercolumnar voids, Figure 2a and highly coherent growth where atomic rows from one columnar grain match precisely the atomic rows of the adjacent columnar grain can be observed, Figure 2b evidencing that PVD coatings with almost bulk material density can be produced when operating at right process conditions.

The peak discharge current density in the HIPIMS process was found to be one of the most crucial parameters that determine all fundamental properties of the films. Detailed discussions on the effects of the significant activation of the deposition flux observed in the HIPIMS discharge on the film texture, microstructure, morphology and properties are

presented elsewhere [21]. This research clearly demonstrated that HIPIMS is a robust tool for structure, texture and therefore coating properties manipulation.

This paper summarises results on the properties and performance of novel nanoscale multilayer structured coatings dedicated to serve in demanding environments. In the following, six strategies are presented to produce such coatings by Direct Current Unbalanced Magnetron Sputtering (DCMS) and High Power Impulse Magnetron Sputtering, (HIPIMS) technologies.

2 Strategies

2.1 STRATEGY 1: Combining elements which produce dense oxide scales with element(s) from the rare earth group, CrAlYN/CrN.

Aerospace and automotive engines represent a particularly challenging area where surface degradation due to environmental attack is the dominant wear mechanism. In recent years various publications showed the potential of monolithically grown TiAlN based coatings to protect cutting tools in dry high speed machining as well as aerospace alloys including Ti-based alloys against oxidation [22-24]. However, the coating structure and the presence of Ti in the coating formula were seen as weak points because Ti forms a large volume porous titania scale which is highly permeable for oxygen especially during exposure to high temperature. Furthermore, as the reported coatings were deposited by the Arc Bond Sputtering (ABS) technique, a major drawback was the presence of a large number of growth defects [25], originating from the droplet phase produced in the arc etching step, which further compromised the coating density. To eradicate these problems a strategy was adopted to develop an Yttrium-stabilised Ti- free nitride based coating utilising nanoscale multilayer structure, where the rare earth element, Y is introduced not only in the bulk of the coating but also in the coating-substrate interface. Furthermore the metals in the coating constitution were selected among those which form dense oxide scales when exposed to high

temperatures. Hence CrAlYN/CrN was developed, [26]. The coating is produced with a nanoscale multilayer structure with a bi-layer thickness of 4.2 nm. HIPIMS was selected as surface pre-treatment, and coating deposition technology to avoid the drawbacks of other state-of-the- art techniques. The utilisation of HIPIMS discharge in the surface pre-treatment stage of the process not only allowed production of a droplet-free ionised metal flux but more crucially allowed implantation of Yttrium in the interface, [27]. It has to be noted that, in contrast to Arc evaporation, HIPIMS allowed the production of Yttrium ions from an alloyed AlCrY target in a very stable process. The Y-stabilised, Ti-free coating formula and the employment of the HIPIMS technology for surface pre-treatment provided the key to enhanced oxidation resistance and stability at high temperature of the coating.

Figure 3a and b show bright field and Z-contrast STEM micrographs of the substrate/coating interface region respectively. The images reveal the entire coating architecture consisting of extremely dense structure of the 200 nm thick CrAlN base layer followed by the nanoscale multilayer CrAlYN/CrN coating. A 5 nm thick band, which changes its contrast from black to white when imaged in bright field or Z-contrast modes respectively indicates the implantation of a relatively heavy atomic weight element at a the fully dense interface.

It has been widely reported that thin films produced by HIPIMS technology can show bulk material density and therefore enhanced oxidation and corrosion resistance, [28]. The effect of the deposition technique on the high temperature performance of the coating is demonstrated in Figure 4. Thermogravimetric analyses of CrAlYN/CrN when exposed to air revealed a significant increase of the temperature for the onset of rapid oxidation up to 950°C for the coatings produced by HIPIMS, as compared to 750°C achieved with coatings deposited by Unbalanced DC Magnetron Sputtering (UBM) technology.

The high barrier properties of the novel CrAlYN/CrN coatings was proved not only in conditions of air oxidation but also in much more aggressive $H_2/H_2S/H_2O$ atmosphere typically found in aero and diesel engine applications.

In the next generation of aero engines, γ- TiAl alloys are seen as a light-weight replacement material to the Ni-based alloys currently used for turbine blades. However, the poor oxidation and sulphidation behaviour of these alloys at high temperatures present a real barrier to their wide application. To assess the potential in turbine blade application, γ- TiAl substrates coated with CrAlYN/CrN were exposed for 1000 h to the aggressive $H_2/H_2S/H_2O$ atmosphere at 750 °C and analysed by thermogravimetry. In these conditions the HIPIMS deposited CrAlYN/CrN were superior to other PVD intermetallic coatings such as Al_2Au and TiAlCr used as a reference and provided reliable protection of the γ-TiAl substrate showing a factor of four reduction in weight gain as compared to the uncoated substrate.

Perhaps the most exciting success of the HIPIMS deposited nanoscale structured CrAlYN/CrN coatings is their fatigue behaviour. In the past the aviation industry has always been cautious with the application of PVD coated components experiencing heavy fatigue load due to the significant fatigue deficit incurred by the presence of the coating. Even the most refined state-of-the-art PVD technologies produce under-dense coatings with a columnar micro-structure which promotes fast incubation and propagation under cyclic load conditions. These cracks then propagate in the substrate material drastically reducing its fatigue stress limit. γ- TiAl substrates coated with CrAlYN/CrN exposed to air at 850°C for 300 h were fatigue tested at room temperature using a stress ratio parameter of R = -1, [29]. The experiments showed that HIPIMS deposited coatings did not deteriorate the ultimate tensile strength of the γ-TiAl substrate. More importantly in the fatigue test HIPIMS coatings showed only 9% fatigue deficit, which can be tolerated by the aerospace industry compared to 20% measured for UBM deposited coatings. This result is believed to be due to the

nanolayered coating architecture, the high coating density achieved by the HIPIMS process as well as the special compositional and structural properties of the coating substrate interface produced by metal ion implantation during the surface pre-treatment stage.

The CrAlYN/CrN showed a peculiar tribological behaviour when tested in the temperature range from 25°C to 630 °C. The increase of test temperature led initially to increase of the steady state coefficient of friction from μ=0.56 measured at room temperature to μ=0.65 at 100 °C followed then by a significant drop to μ=0.4 at 650 °C. Such behaviour is in stark contrast with the behaviour of Ti containing coatings such as TiAlN and TiAlCrYN which in similar test conditions showed steady increase of the friction coefficient to values above μ=1.0 at 650 °C due to significant material transfer during sliding. The low friction coefficient of CrAlYN/CrN at high temperatures can be attributed to the formation of Cr_2O_3, eskolite found in the wear track by Raman spectroscopy. Eskolaite has hexagonal close-packed (h.c.p.) lattice, where each metal site is surrounded by an oxygen octahedron, which is typical of many so-called Magnéli phases that are known for their solid lubricant properties [30].

The synergy between excellent oxidation resistance, low coefficient of friction at high temperatures and high hardness (40 GPa) retention up to 950°C is best demonstrated for CrAlYN/CrN in dry high speed machining operations. In dry high speed milling at cutting speeds of v_C =385 m min^{-1} of hardened A2 tool steel (HRC=58), 8 mm cemented carbide ball nosed end mills coated with CrAlYN/CrN outperformed a range of advanced PVD coatings including TiAlCrYN, which is one of the market leading coatings dedicated to this application. When the test was carried out at the higher end of the cutting speed range of 500 m min^{-1} this difference in performance became even more pronounced where CrAlYN/CrN coated tools showed a factor of 8 longer life time.

The excellent high temperature stability, enhanced tribological performance as well as reliable barrier properties against environmental attack rank CrAlYN/CrN as a potential candidate to protect turbine blades or applied on hot rolling or forming dies, Figure 5 a, b.

2.2 STRATEGY 2: Utilisation of Magnéli phases formed in-situ at the asperity contacts during sliding.

Following this strategy, TiAlN/VN has been designed as a wear resistant coating, for broad scale tribological applications such as protection of cutting tools and machine wear parts. The strategy to improve the wear resistance of nitride based ceramic coatings namely TiN by the incorporation of further elements in the form of metals (Al, Zr) or metalloids (C, O) was adopted in the early 1980s, [31, 32]. The incorporation of Vanadium to produce a stable (Ti, V)N phase resulted in superior wear resistance, [33]. In these early years of research however, the improved wear performance was attributed to the structure refinement and the associated enhanced mechanical properties such as hardness. The effect of the formation of solid lubricants due to tribochemical reactions in the sliding contact in dry sliding conditions was realised at a later stage, [34, 35]. In the case of V- containing coatings a significantly lower coefficient of friction can be achieved due to the formation of V_2O_5 promoted by the high flash temperatures (up to 800°C) at the asperity contacts during sliding wear. V_2O_5 belongs to the family of the ***Magnéli*** phases, which contain easily shearable crystallographic planes and therefore enhanced lubricity. Furthermore the low melting point of the oxide, T_m=681°C is typically exceeded at the asperity tribological contacts and therefore effectively the sliding takes place in the presence of material in a liquid state, which further reduces the friction. This effect has been clearly demonstrated by thorough differential scanning calorimetry (DSC) combined with SEM investigation of the morphology of the wear track in high temperature pin-on-disc tests, [36].

One prominent drawback of the monolithically grown V- base nitrides reported by many researchers is their high brittleness, [32, 37]. The enhanced mechanical properties of the superlattice structured coatings have been well known from the onset of their development. Recently, similarly to the superhardening effect, fracture toughness enhancement as a function of the bi- layer thickness has also been demonstrated [38]. Based on this knowledge, a strategy was adopted to combine the highly abrasion resistant TiAlN with the ***Magnéli*** phase to form friction- reducing VN in a TiAlN/VN coating utilising a superlattice structure to serve as a wear resistant coating for a broad range of tribological applications including protection of cutting tools and machine wear parts.

The low magnification XTEM image in Figure 6a shows the coating architecture consisting of a dense 0.25 µm thick TiAlN base layer followed by the TiAlN/VN nanolayer stack. The superlattice structure consisting of sequentially deposited TiAlN and VN are resolved at high magnification (Figure 6b).

The excellent wear behaviour of TiAlN/VN in dry sliding conditions has been widely reported elsewhere [39, 40]. However, the exceptionally low wear coefficient of $1.26.10^{-17}$ m^3 N^{-1} m^{-1} determined in a pin-on-disc test after a sliding distance of 70 km is difficult to attribute to the superhardness (42 GPa) alone or to the distinctive nanoscale layer-by-layer wear mechanism which is characteristic of superlattices and arises through the presence of crack deflecting interfaces in the coating structure. A thorough investigation of the worn surface involving characterisation of the phase composition of the wear debris by Raman spectroscopy,[35] chemical composition analyses by TEM-EDX and Electron Energy Loss Spectroscopy (EELS) as well as XTEM imaging of the worn surface, [41] contributed to the better understanding of the wear mechanisms involved. It was found that during dry sliding a 20-50 nm thick tribo-film forms, which is well adhered to the worn surface. Figure 7 shows a XTEM image of the tribo-film formed in the wear track during a pin-on disc dry sliding test.

The EELS analyses revealed that the tribo-film contains Me-oxides formed through a tribo-oxidation mechanism whereas the Raman spectroscopy clarified specifically the formation of the lubricious V_2O_5. The detailed TEM imaging, electron diffraction and EDX analysis revealed that the tribo-film is amorphous and has a clear boundary to the adjacent TiAlN/VN coating. In stark contrast to monolithically grown nitrides with columnar structure where severe bending and fracture of the top of the columns is observed to take place during sliding, the TiAlN/VN coating at the worn surface cross-section edge showed a high structural integrity and was free of any visible cracks or deformation. This effect is believed to be due to the lamellar structure of the coating and the presence of a tribo-film based on a ***Magnéli*** oxide phase, which reduces the severity of stress concentration by redistributing the sliding contact stresses.

The consistently low and almost temperature-independent coefficient of friction recorded for room and elevated temperatures is big advantage for TiAlN/VN. However, due to the poor oxidation resistance of Vanadium the coating application is limited to the moderate temperature range, (below 800°C-850°C) which is typical for tapping operations as well as machining of softer materials e.g. stainless steel or Ni-based alloys.

A modified version of the TiAlN/VN superlattice coating with added 2% Y to enhance the coating stability at higher temperatures showed excellent performance in milling of low-alloyed steel where the temperature during machining can exceed 900°C. Solid carbide two flute ball-nosed end mills, 8 mm in diameter, were coated with a TiAlYN/VN superlattice coating, and compared with a monolithically grown TiCN coating when dry cutting EN24 steel, HRC 38. The cutting conditions were as follows: a cutting speed of 385 m min^{-1}, a feed/revolution of 0.2 mm, and an axial depth of 3.8 mm. In these conditions, the uncoated tool showed a tool lifetime of only 7 min, the commercially-available TiCN coated tools increased the lifetime to 53 min, whereas the TiAlYN/VN superlattice coating tripled the

lifetime compared to TiCN, thus demonstrating the advantages of the superlattice structured PVD coatings.

Another demanding application where TiAlN/VN superlattice coatings have great potential is in the machining of tough materials such as Inconel and stainless steel. TiAlN/VN-coated 8 mm two-flute ball-nosed end-mills were tested in dry cutting of Inconel 718, HRC 43, cutting speed 90 m/min, axial depth of cut 0.5 mm, feed 0.2 mm. The superlattice coated tools, photographed in Figure 8a, showed the longest length of cut of 380 m, out-performing various PVD coatings: TiAlN, TiAlN+WC/C, TiAlN+ MoS_2, TiAlN+Graphite, Figure 8b.

2.3 STRATEGY 3: Utilisation of Low Shear Strength Interfaces produced by dynamic segregation of small atomic radius elements such as Carbon.

As postulated, the hardening effect in superlattice structured coatings has been attributed to the role of the interfaces as barriers to dislocation movement. Furthermore sharp interfaces are regarded as a prerequisite for a coherent film growth and therefore higher hardness. However, it has been reported that in industrial PVD coatings their interface width exceeds 1 nm, [42] which represents a substantial fraction of the volume of the nanoscale multilayer stack, whose typical bi-layer thickness is 2–5 nm. It is logical to expect that the relatively disordered structure of the interface would provide conditions for easier diffusion paths or accumulation of elements such as C, which has a small atomic radius and therefore a high mobility. Migration of C during coating growth has already been shown to take place in non-reactively sputtered Me–C films grown in conditions of high ion irradiation [43]. This suggests that under certain conditions the interfaces between the individual layers in the nanolayered coating could be compositionally modified and enriched with a specific element. Strategy 3 of this publication constitutes a microscopic enrichment with carbon to reduce the shear strength of the interfaces and change the wear mechanism of the material which dramatically influences tribological properties.

Following this strategy, TiAlCN/VCN nanostructured coatings were produced. High magnification bright field imaging showed the nanoscale multilayer structured coating architecture with a period of 2.2 nm (Figure 9a). Careful analysis of this image reveals that in the growth direction a bright contrast phase is segregated at the interfaces between the individual layers of the multilayer stack thus forming an additional bright contrast layer within each period.

EELS line scans across the layers were carried out on a scanning TEM (STEM) type JEOL 2010F operating at 200 kV and a probe size of 0.18 nm. The distribution of the coating elements including C, V, Ti and N was recorded and is presented as normalised line scans (Figure 9b). The STEM-EELS analyses confirmed that C is accumulated at the interfaces between the individual nanolayers. The highest intensity of the C spectra appears in between the V-rich and TiAl-rich layers. This particular structure, where the C is segregated vertically is favoured by the presence of interfaces between the individual nanolayers which provide sites for preferential accumulation. The segregation in the growth direction of carbon in nanolayered structures such as TiAlCN/VCN is a reproducible process. Formation of low shear strength, ("slippery") interfaces due to dynamic segregation of carbon during coating growth has also been realised with the CrAlCN/CrCN system, [44].

Key industries such as aerospace, automotive and medical use extensively Al, Ti and Ni-based alloys. These materials are softer than hardened steels but react metallurgically very strongly with the cutting tool. The reaction builds up material on the cutting edge and makes high speed machining problematic. One immediate approach to eradicating this problem is the application of coatings to limit the reactivity of the surface of the cutting tool. However, it has proven extremely difficult, if not completely impossible, to find a coating material, which is fully inert. For example, diamond-kike carbon (DLC) coatings show excellent inertness to Al but would react with Ti. A solution to this problem has been achieved through a coating

architecture, which is designed to change the wear mechanism of the material rather than prevent the metallurgical reactions in the tribocontact.

TiAlCN/VCN coatings utilising low shear strength ("slippery") interfaces have shown very promising performance in preventing the build-up edge formation. XTEM carried out on the worn surface of TiAlCN/VCN after pin-on-disc tests showed the absence of tribofilm even after sliding distances of 12 km [45]. This is in stark contrast with the behaviour of the C-free version of the coating. The suppression of the tribofilm effectively inhibits the formation of thick built up layers during cutting, which increases the tool life time.

A schematic illustration of the wear mechanisms of Carbon-free and Carbon-containing coatings is shown in Figure 10 [46].

The advantage of low shear-strength interfaces can be understood by identifying the position of the coating delamination interface during operation. When the interfaces have a high shear-strength as in TiAlN/VN, the coherent coating growth provides a strong interface bonding between the individual layers and the wear resistance against inert ceramics is extremely high. However, during cutting, the coating forms a 10-20 nm thick tribo film [41] which is sufficiently strong as to support a thick build up layer on top due to the metallurgical reaction with the work piece material. The weakest interface in this case is positioned between the coating and the tribofilm. When eventually the build-up becomes excessive and does delaminate, a large volume of coating material of the order of several thousands of nm^3 will be lost resulting in a high wear rate. In contrast, the delamination interface in TiAlCN/VCN is positioned within the carbon layer which is segregated within the top few nanometres of the tribological surface thereby preventing both tribofilm formation (as confirmed by XTEM [45]) and thick build up layer formation [46, 47]. In this case low wear rate is achieved due to the change of the wear mechanism of the material to a well-defined layer -by-layer wear on the nanometer scale.

The excellent performance of TiAlCN/VCN has been demonstrated in machining of a number of difficult to machine Al- and Ti- based alloys as well as Metal Matrix Composite (MMC) materials. In dry milling of aerospace grade Al 7010-T 7651 alloys, TiAlCN/VCN nanoscale multilayer PVD coatings outperformed state of the art DLC, Cr/WC/a-CH coated and uncoated end mills by factors of 4 and 8 respectively [46]. According to independent tests performed at Airbus, TiAlCN/VCN coatings are ranked as the preferred candidate for dry high speed (> 24 000rpm) machining of Al7010 alloys, used for the wingbox rib of an A380 airplane shown in Figure 11a [47].

In turning tests on Ti alloys (TiAl6V4) conducted at Symmetry Medical Sheffield Ltd. in the UK, TiAlCN/VCN-coated cemented carbide inserts produced a factor of two to three more components (orthopaedic implants, Figure 11b), as compared to uncoated tools [46]. Cutting tests carried out at the Fiat Research Centre in milling TiAl6V4 alloys showed a life time improvement by factor of 6 as compared to uncoated tools and an improvement of almost a factor of 2 over DLC-coated tools. Thermocamera measurements of the temperature developed in chips revealed that the control temperature of 800°C was achieved with TiAlCN/VCN after 65 m cutting length compared to 45 m for DLC coated and only 10 m for the uncoated tools [47].

Hydra Clarkson International Ltd., Sheffield, UK single or combination drills coated with TiAlCN/VCN have been successfully used to machine various grades and combinations of composite sheet material. The composite sheeting was 8 mm thick comprising a synthetic top and bottom layer and several aluminium and synthetic middle layers. In these conditions, the PVD-coated drills produced 130 holes compared to only two holes produced by the uncoated drills [48]. The TiAlCN/VCN coating solution was patented by Sheffield Hallam University, UK in 2005 [49].

2.4 STRATEGY 4: Utilisation of high ion irradiation to achieve phase separation and formation of self-organised nanostructures in metal - doped Carbon films.

DLC and pure carbon coatings often suffer from poor toughness and brittleness due to high compressive residual stress. These deficient properties have been improved by doping the carbon coating with a small amount of more ductile metals, e.g. Cr, Ta, W or Ti. Further improvement was achieved by utilising multilayer structures, which also allowed the selection and combination of materials according to the desired properties. Multilayer C/Cr coatings, registered as Graphit-iC™ produced by unbalanced magnetron sputtering are amongst the best representatives of this approach [50]. The concept of advanced nanolaminated PVD coatings combining the advantages of both the concepts of carbon-based nanocomposite coatings and those of multilayer coatings has first time been described in [51]. These novel nanoscale single-layer composite coatings composed of coexisting metastable hard phases like fcc (Ti,Al)(N,C) and amorphous carbon grown by magnetron sputtering have shown promising properties and performance both in laboratory tribological testing as well as in tool testing.

Considerable interest in the research of thin carbon films arises from the possibility of changing the film properties, by tailoring the microstructure, i.e. from graphite-like to diamond-like with an amorphous or crystalline structure, and the variation in sp^2 / sp^3 ratio by proper selection of the deposition conditions and techniques [52]. It is well known that the energy of ion bombardment and the ion to- neutral ratio during the film growth strongly affect the growth, structure, and thus the properties of the coatings. For carbon nitride (CN) thin films, for example, it has been shown that coating growth in conditions of low ion irradiation (bias voltage from -25 V to - 40 V) leads to deposition of smoother films, changes in the degree of curvature of the graphitic sheets, extent and alignment of the microstructure and results in improvement in strength, toughness and elasticity of the coatings [53].

The availability of independent control over the energy, E_i and relative flux, J_i / J_n of the bombarding ions in modern PVD systems, provides a powerful tool for structure tailoring [54] and for self-organised growth in particular. Self- organised structures evolve usually in multicomponent, multiphase thin films or films with artificial structures such as nanoscale multilayers or nanophase composites produced in deposition conditions far from thermodynamic equilibrium. A typical example is the formation of the so-called tissue phase in composite coatings, which covers the grain boundaries of film grains [55]. The tissue phase develops during film growth by a self-controlled kinetic segregation of active additives and repeated nucleation mechanisms, which in combination define the coating structure. The Me- Carbon is another system which provides unique material for development of self-organised structures.

It is anticipated that due to the very low elemental sputtering yield of C (sputtering yield for 500 eV Ar^+ ions of 0.12 for C and 1.18 for Cr [56]) the films will grow under conditions of intensive ion bombardment (high ion to neutral ratios). Indeed, for the deposition in fairly standard conditions for magnetron sputtering of Carbon, ($U_{cathode}$ = - 600 V, Power density, W_c= 3 Wcm^{-2}) and relatively low bias voltages (U_b = -75V) an average ion flux to the substrate of J_i of 5.6 × 10^{15} ions $cm^{-2}s^{-1}$ and neutral deposition flux of J_n of 1.07x10^{15} atoms $cm^{-2}s^{-1}$ have been measured, showing that the condensation of the film takes place at a very high J_i/ J_n ratio of 5.2 [57]. These observations allowed the formulation of Strategy 4 in the current publication, namely: Utilisation of high ion irradiation to achieve phase separation and formation of self-organised nanostructures in Metal (Me)- doped Carbon films**.**

Cr-doped Carbon films have provided an example of the effect of self-organised growth on the structure, properties and in-service performance of Strategy 4 coatings [43]. C/Cr coatings were deposited by non-reactive unbalanced magnetron sputtering utilising three graphite and one Cr target at a wide range of bias voltages, U_b, between - 65 and - 550 V.

Plasma diagnostics carried out by electrostatic probe measurements revealed that C/Cr films grow under conditions of intensive ion bombardment with ion-to-neutral ratio $J_i / J_n > 6$. Under these conditions the high diffusion mobility and the reactivity of the C leads to distinct changes in the coating microstructure and phase composition.

High-resolution transmission electron microscopy (HRTEM) employing high-angle annular dark field (HAADF) imaging revealed that the microstructure evolved from columnar with carbon accumulated at the column boundaries for U_b = - 65 V and - 95 V, (Figure 12a) to a structure dominated by "onion- like" C–Cr clusters at U_b = - 120 V, (Figure 12b). The curved shape of the C- Cr clusters often referred to as "onion-like" structure is due to the bending of the carbon planes when metal atoms are introduced in the graphite lattice. At higher bias voltages, U_b = - 350 V and - 450 V the structure subsequently converts to a distinct nanoscale layered structure as shown in (Figure 12c).

The new nanoscale layered structure is characterized by values for the bi-layer thickness of 20 nm and 25 nm, for films grown at U_b = - 350 V and U_b = - 450 V respectively. This average periodicity is an order of magnitude larger than that calculated on the basis of the total deposition thickness and sample rotation frequency. It is believed that the formation of this new type multilayer structure with abnormally large periodicity occurs via a segregation and self-organisation mechanism triggered by the high-energy ion irradiation of the growing film.

The reproducibility of these structures and the processes behind them have been demonstrated by a simple experiment, where the bias voltage to the substrate during coating deposition was altered from low (U_b = - 75 V) to high (U_b = - 350 V) in four cycles. A BF XTEM image of the overall structure of the coating is shown in Figure 13a. On top of the 250 nm thick CrN base layer one can clearly see four pairs of layers containing both representative structures in their finest details. In each cycle the low energy irradiation has

produced a columnar structure with column boundaries enriched in C and rough top surface of the coating. In contrast high-energy irradiation has resulted in a precise layered structure, in which carbon-rich clusters (showing white contrast areas) are aligned in layers surrounded by a metal rich matrix (see areas with darker contrast). A higher magnification image of the clusters is shown in Figure 13b.

Annular dark field (ADF) STEM imaging and quantitative EELS analysis showed that the nanoscale multilayer structure comprises of alternating layers of a Me-carbide phase (48%C, 52%Cr) and clusters of almost pure C (91.34%C). Raman, XPS and EDX analysis for coatings grown at U_b = - 350 V further revealed that the Me-carbide phases formed are namely Cr_3C_2 and/or Cr_7C_3.

A coating growth model has been proposed which details the role of irradiation-induced ion mixing, re-sputtering, condensation surface temperature effects, nucleation and kinetic segregation process, as well as the diffusivity of the coating elements in accounting for the phase separation and formation of the self-organised layered nanostructure observed in C/Cr coatings [43].

The mechanical and dry-sliding tribological properties of C/Cr films are influenced by the ion irradiation conditions [58]. The lowest coefficient of friction of $\mu = 0.16$ and lowest wear coefficient of 6.75×10^{-17} $m^3N^{-1}m^{-1}$ have been achieved with conditions of ion bombardment corresponding to a bias voltage of U_b = - 95V. C/Cr coatings produced at higher bias voltages, (U_b = - 350V) show increased coefficient of friction of $\mu = 0.31$ and wear coefficient of 3.02×10^{-16} $m^3N^{-1}m^{-1}$. However, the unique structure of these coatings comprising a hard metal carbide matrix with embedded lubricious C-rich clusters proved to be very advantageous in applications such as wear protection of precision blades.

One such specialised niche application is surgical blades. Scalpel blades coated with C/Cr produced in conditions of high irradiation (U_b = - 350V) have been tested at Swann Morton

Ltd., Sheffield, UK using specialised equipment and procedures. The cutting efficiency of the blades was defined by the number of the cutting strokes needed to cut through 5.35 mm diameter rubber material under constant normal load. The number of repeat cycles in this type of test is indicative of the long- term performance or the useful life-time of the cutting edge. The result from the first cutting trial is indicative for the initial sharpness and the wear resistance of the surgical blade. Deposition of C/Cr PVD coatings at optimised conditions on surgical blades reduced the number of the cuttings strokes to the range 3-5, thus demonstrating improvement of the cutting performance of factor of 5 compared to that of the untreated blades.

Similarly significant improvement in the cutting performance was achieved with high irradiation C/Cr coated razor blades. The technique allowed the deposition of high aspect ratio, low friction coatings creating a sharp but robust cutting edge, which resulted in the reduction of the cutting forces by a factor of five and increased the life-time of the cutting edge by a factor of three. It has to be noted that in this application the applied bias voltage is one of the most powerful process parameters, which defines the cutting edge geometry. Hence for an enhanced performance it is imperative that the right balance between coating structure, composition, adhesion properties and correct tip geometry is achieved. Low and high magnification XSEM images show the excellent tip coverage as well as the well-preserved sharpness of the cutting edge after the deposition of the high irradiation C/Cr coating (Figure 14 a, b).

2.5 STRATEGY 5: Utilisation of tribo- chemical reactions to achieve" in-situ" formation of lubricious phases in conditions of boundary lubrication in Me- doped Carbon films.

Simultaneous doping of Carbon coatings with W and Mo allowed production of low-friction and low-wear tribological coatings to operate in boundary lubricated conditions at elevated temperatures (>200 °C).

Metal-free and metal-doped DLC coatings are extensively used as tribological coatings for engine parts due to their excellent combination of low friction and improved wear resistance properties. But it is quite challenging to use DLC on components, which are operated in conditions where the temperature, load and sliding velocity are high as in the piston-cylinder and the valve-train assemblies, where the maximum operating temperature typically ranges between 150°C and 300°C [59]. It is well understood that DLC coatings show low friction and high wear resistance at ambient temperature due to the formation of a graphitic tribolayer at the asperity contacts [60]. With the increase of test temperature (100–300°C) however, both graphitisation and oxidation of DLC coating degrade its properties leading to a substantial increase in both friction and wear coefficients [61].

In lubricated sliding, several approaches have been explored to achieve enhanced performance of the DLC coatings. One such approach is to manipulate the chemistry of the lubricants used to form highly lubricious tribolayers during sliding. For example, some of the state-of-the art formulated engine oils contain anti-wear (AW) additives such as Zinc dialkyl dithiophosphate (ZDDP), extreme-pressure (EP) additives and friction modifiers such as molybdenum dithiocarbamate (Mo-DTC). During sliding, Mo-DTC is thermally decomposed forming a tribolayer containing MoS_2, which significantly reduces the coefficient of friction [62].

Another approach for further reduction of the friction is doping DLC with different metals. For example, the RF magnetron sputtered Ti-DLC and Mo-DLC coatings showed much lower friction ($\mu \sim 0.03$ and $\mu \sim 0.05$–0.1 respectively) compared to metal-free DLC coating ($\mu \sim 0.2$) when SAE 5W-20 formulated engine oil (contains polyalphaolefin, ZDDP and Mo-DTC) was used as lubricant. The low friction of Ti-DLC and Mo-DLC coatings was attributed to the formation of high strength metal carbides in the defective parts of the carbon

network and formation of MoS_2-containing tribolayer due to thermal decomposition of Mo-DTC [63].

Similar to ambient temperature, the formation of a MoS_2-containing tribolayer in the temperature range of 50–100°C decreases the friction coefficient ($\mu \sim 0.02–0.14$) of various metal-doped (such as Si-doped, Ti-doped and W-doped) DLC coatings under different test conditions [64].

However, with further increase in test temperature to 200°C and above, all the coatings discussed above significantly increase their friction and wear rate due to degradation of their properties. Therefore, these coatings could not be classified as suitable for components used in high temperature applications and further research was needed to provide solution for this demand.

Strategy 5 described in this work aimed at the utilisation of tribo- chemical reactions to achieve "in-situ" formation of lubricious phases in conditions of boundary lubrication in Me-doped Carbon films. Following this strategy a carbon-based coating which is simultaneously doped with Mo and W was developed.

Unlike the state-of-the-art coatings where the formation of the lubricious metal chalcogenides, (MoS_2 and WS_2) occurs due to thermal decomposition of the various types of oil additives used in Strategy 5 coatings form lubricious phases "in situ" via tribochemical reactive processes taking place at the asperity contacts. In this case the high flash temperatures (exceeding 800°C) in the asperity contact during sliding trigger reactions between the Mo and W dopants in the coating with Sulphur, which is a natural ingredient of the oil to form lubricious MoS_2 and WS_2 compounds. The advantages of this approach are that the solid lubricant is produced right at the asperity contact where it is most needed and that the process is effective even with non-formulated oils. Furthermore, the addition of doping elements such as Mo and W into the Carbon coating delays the graphitisation process

and therefore is seen as a resourceful approach for the preservation of coating properties at higher temperatures.

The Mo- and W- doped Carbon coatings were deposited by a hybrid HIPIMS/ UBM process in non-reactive Ar atmosphere [65]. The coating architecture consists of a HIPIMS-engineered interface, a Mo–W–N base layer and a Mo–W–C top layer. The coating showed high adhesion with substrate (scratch adhesion test critical load L_C > 80 N) and a moderate hardness of 17 GPa.

The XSEM image in Figure 15a shows the overall coating architecture and reveals the high coating density and smooth surface due to the employment of HIPIMS. The coating has a pronounced nanoscale multilayer structure as imaged by TEM, Figure 15b.

Lubricated sliding pin-on-disc tests carried out under 5 N load at ambient temperature (~30°C and ~30% relative humidity) using 100Cr6 steel ball counterpart and highly viscous Mobil 1 Extended life^{TM} 10W-60 synthetic engine oil revealed the excellent tribological behaviour of the Mo–W–C coating with a mean friction coefficient as low as μ = 0.033 and no measurable wear after a sliding distance of 7500 m. Raman spectrum collected from the wear debris within the wear track indicated the presence of metal carbides, (WC, Mo_2C, etc.), graphitic Carbon and, importantly, metal sulphides - mostly WS_2. When the test temperature was increased to 200°C the coefficient of friction marginally increased to μ = 0.056 and formation of wear debris containing large amount of MoS_2 was also detected by Raman analysis. A Raman spectrum and associated optical micrograph of the wear debris produced during lubricated sliding at a high temperature of 200°C on the steel ball counterpart are shown for two different positions in Figures 16a and 16b.

The results unambiguously demonstrate the "in- situ" formation of the lubricious MoS_2 and WS_2 compounds in boundary lubricated sliding conditions of Mo-W-C coatings due to chemical reactions taking place at the asperity contacts of the tribo-couple. In comparison

Raman analyses of the wear debris of commercially available hydrogenated DLC coating tested in similar conditions showed only the presence of graphitic material which confirmed that in this case a simple graphitisation process is responsible for the poor performance of this coating at elevated temperatures. This striking difference in the tribological behaviour of the Mo-W-C coatings and pure DLC coatings at elevated temperatures, (200°C) is demonstrated in Figure 17, which compares the coefficient of friction curves recorded in a lubricated pin-on-dick test. It can be seen that in the condition of this test the Mo-W-C coating gradually reduces (improves) its coefficient of friction due to a continuous formation of lubricious MoS_2 and WS_2 compounds, whereas the pure DLC coating progressively increases (deteriorates) its coefficient of friction due to the progression of the graphitisation process at the elevated test temperature.

The high thermal stability of the Mo-W-C coatings was demonstrated in dynamic oxidation tests by Thermogravimetric Analyses (TGA) [67]. In these tests no change in mass up to a temperature of ~600°C was recorded, and only a slight increase in mass gain to ~3 mg when heated up to ~800°C was measured. In comparison, DLC coatings showed spallation and rapid oxidation after 350°C. In static oxidation tests, Mo-W-C coatings exposed to 500°C in air for 1 hour showed no spallation or coating surface degradation. SEM image of the exposed surface is shown in Figure 18a. On the other hand, DLC coatings tested in similar conditions were completely evaporated and exposed the substrate as shown in Figure 18b.

Mo-W-C coatings have been successfully deposited and tested on a number of automotive components such as piston rings and tappets, Figure 19 a and b respectively.

The Mo-W-C coating solution was patented by Hauzer Techno Coating B.V. and Sheffield Hallam University in 2014 [68].

2.6 STRATEGY 6: Combining highly wear resistant with electrochemically stable elements to achieve corrosion and wear resistant coatings, CrN/NbN.

The main aim of combining Nb and Cr in a superlattice coating of CrN/NbN was to produce an environmentally friendly replacement for hard chromium. The rationale behind selecting NbN was to utilise the excellent corrosion resistance of the electrochemically-stable Nb, whereas CrN has been chosen to enhance wear resistance and allow low deposition temperatures (~200°C) with a good adhesion. The aim was that the combined enhanced corrosion resistance and super-hardness (Plastic Hardness, HP = 40 GPa) would lead to a new PVD product with a thickness of 4-5 µm and wear performance equivalent to that of electroplated Cr coating with thickness of 20 µm and hardness of 1 GPa.

CrN/NbN superlattice coatings have been deposited by sputtering of two adjacent pairs of Cr and Nb targets with purity of 99.8% in a mixed Ar and N_2 atmosphere. Depending on the application either Cr^+ or Nb^+ ion etching has been employed followed by deposition of a 0.3 µm CrN base layer and deposition of the 4-5µm CrN/NbN superlattice coating with a superlattice period Δ = 3-4 nm. To suit a range of substrate materials and the applications, two types of processes have been developed: utilising low deposition temperatures of 250°C and high deposition temperatures of 450°C. XTEM micrographs illustrating the structure of CrN/NbN are shown in Figure 20 a, b**.**

The first detailed results on the tribological [69] and corrosion performance [70] of CrN/NbN deposited by the combined Arc Bond Sputtering (ABS) technique were reported in 1999. This research has been later progressed to involve Cathodic Arc Evaporation [71] and HIPIMS [72, 73] techniques. High hardness of 35 GPa excellent tribological performance and corrosion resistance was achieved already with the ABS and Arc deposited coatings. For example ABS CrN/NbN coatings when deposited on 304L Stainless Steel substrate withstand 1500 hours in salt spray test and 300 hours when deposited on Mild steel, which exceeded the life time required by the industrial standard for electroplated hard Chromium coatings.

However, the presence of macroparticle (droplets) or macroparticle-promoted growth defects in the structure of the Arc and ABS coating presented a great challenge to the corrosion resistance of the CrN/NbN films.

The effect of the deposition method on coating density is demonstrated by the XSEM images in Figures 21a, 21b, and 21c. A droplet defect typical for the Arc deposition method with a diameter of ~ 2 μm is captured on the focussed ion beam (FIB)-XSEM image in Figure 21a. The droplet has been deposited on the substrate surface at the initial stages of the coating growth creating an under-dense volume of coating material on its top separated from the main coating by a clearly visible gap. A similar defect structure is observed with the ABS coatings where the arc technology is used in the substrate pre-treatment stage where as the coating is deposited by magnetron sputtering, Figure 21b. Droplets are pure metal macroparticles emitted by the cathode spots in the Arc discharge. When embedded into the coating material droplets not only deteriorate the coating density but importantly they also compromise the electrochemical stability of the material due to the significant difference between the corrosion potentials E_{corr} of the droplet material (pure metal) and the surrounding coating (ceramic material, in this case Nitrides of Cr and Nb). Potentiodynamic polarisation measurements in NaCl water solution for Cr-CrN system for example showed that $E_{corr.}$ of Cr is -587.78 mV compared to E_{corr} of -202.67 mV measured for CrN, [74]. In wet corrosion environments, this large potential difference accelerates the corrosion damage due to the electro-chemical dissolution of the droplet material.

Further improvement in the corrosion resistance of CrN/NbN was achieved by the utilisation of the HIPIMS deposition process, which produces highly dense, free of droplet macroparticles coatings as shown in the XSEM image in Figure 21c.

Table 1 summarises the properties of electroplated Hard Chrome and CrN/NbN deposited by ABS and HIPIMS technologies. It illustrates the excellent corrosion and tribological

performance of the nanoscale multilayer coating and the advantages when deposited by the novel HIPIMS technology, [73, 75]. These results show that CrN/NbN can be regarded as a true green alternative to the Cr plated coatings.

The synergy between excellent corrosion resistance and enhanced tribological performance has opened up a wide field of application for CrN/NbN. The coating has been successfully applied and tested on various components for textile machines processing extremely aggressive (high wear and corrosion) polymeric fibre. Combing rollers for Rotor spinning, textile scissors and blades have been tested by Schlafhorst, Germany demonstrating a step improvement in the component in-service lifetime [76]. Another promising field of application is the cutlery industry and protection of surgical blades where CrN/NbN outperformed coatings such as CrN, DLC and plasma surface treated (nitrided) blades [77]. The low magnification SEM and XTEM images in Figure 22a, b show the high thickness uniformity as well as the development of the superlattice structure with a high precision of the coating on the sharp edge of a scalpel blade.

CrN/NbN has been implemented in large scale production by Lafer Spa, in Italy. Various types of components such as plastic moulding, metals minting, polyurethane molding of epoxi resins, thermoset molding and others are coated on commercial bases. Some examples are shown in Figures 23a, 23b and 23c.

The demand for new materials to be used in supercritical steam power plants for efficient and clean coal utilization is ever growing. A significant reduction of CO_2 emissions is expected by increasing the efficiencies of the steam turbines to s > 50% which can be achieved by moving from subcritical conditions (180 bar/540°C) to an ultra-supercritical regime of operation (300 bar/620 - 650°C). However, turbine components face various challenges, related to higher temperatures such as material failure due to high temperature oxidation, and phenomena such as creep and erosion caused by descaled fragments. Until recently the PVD

route has not been exploited for this application. The main reason being the porous structure of the state-of-the-art coatings, especially when monolithically grown, inherent to their growth mechanism. However, HIPIMS deposited CrN/NbN coatings with hardness of 35GPa, Young's modulus of 440 GPa and very high adhesion of L_c= 80N utilising nanoscale multilayer structure deposited on P92 steel have shown a promising performance when subjected to various types of high temperature tests in an aggressive pure steam environment [78, 79, 80].

CrN/NbN coated P92 turbine steel substrates were oxidised at 650°C in 100% steam atmosphere up to 2000 h, in order to simulate the future operation conditions of steam turbines employed in power plants. In these conditions a mere 490 nm of protective scale comprising Cr_2O_3 and NbO was sufficient to stop degradation and Oxygen was not detected either in the bulk of the coating or at the coating-substrate interface as evident from the XSEM image and the corresponding EDX analysis results (Figure 24). The oxidation kinetics revealed by thermogravimetric analysis at the conditions of the experiment showed negligible mass gain for the CrN/NbN coated P92 steel compared to 23 $mgcm^{-2}$ measured for the uncoated substrate.

The effects of the CrN/NbN coating on the mechanical properties of the P92 steel substrate were extensively tested at an elevated temperature of 650°C in a battery of tests including Ultimate Tensile Strength, Low Cycle Fatigue, and High Temperature Creep. The results are presented in Figures 25a, 25b, and 25c. It can be seen that the HIPIMS-deposited CrN/NbN not only retains the mechanical properties of the P92 substrate material but in some cases a significantly improves the Ultimate Tensile Strength and time to fracture in High Temperature Creep test [57].

Turbine blades are subjected to severe water droplet erosion. In aviation studies, for the case of water droplet erosion, the parameter 'Damage Threshold Velocity (DTV)' represents the

lowest velocity, which could theoretically cause damage in the target material. The theoretical description for the DVT, (not shown here) clearly defines the fracture toughness and hardness as two of the most influential material properties for high water droplet erosion resistance. The synergy between superhardness and a special crack propagation mechanism rank the superlattice structured materials amongst the toughest PVD coatings. In the case of CrN/NbN excellent water droplet erosion resistance was demonstrated in a water droplet erosion test, using a test rig from RFT Germany. In this test no measurable coating weight loss was detected after 2.4×10^6 impacts at a pressure of 9 bar. The surface morphology after the erosion test resembled largely the original morphology. A 2D surface plot (Figure 26a) revealed a formation of a shallow circular depression at the targeted surface area. Using 3D scanning profilometry (Figure 26b) the depth of the depression was measured to be about 20 µm. It is believed that the depression was formed due to deformation of the substrate material beneath the area of the sample impacted by the water jet. However, importantly no coating delamination or cracks were observed by post-test SEM imaging, which demonstrated the exceptionally high coating adhesion, high impact load resistance and high impact fatigue resistance in particular of the coating achieved by the HIPIMS technology. This pioneering research leads to the assumption that the synergy between advanced coating nanostructure, appropriate coating material selection and the application of the High Power Impulse Magnetron Sputtering deposition technology projected CrN/NbN as a potential candidate for the protection of steam turbine blades against environmental attack as it possesses the whole package of functional properties required for this application.

Perhaps one of the most exciting successful applications of the Strategy 6 CrN/NbN coatings is the one in the medical orthopaedic implant sector. Human joints are bearings and as such joint replacements must be manufactured from materials that display good biocompatibility and also enhanced tribological properties in order to ensure long-term clinical performance.

The most widely used bulk metallic materials for implant components are CoCrMo alloys and surface-treated Ti-6Al-4V alloys; however these materials present certain limitations themselves [81]. Therefore various types of PVD coatings have been investigated and some of them commercially used namely TiN, CrN, ZrN, CrCN, DLC and others. Despite the multitude of coatings that have been presented, the main concern with these has been the adhesion to the substrate. Furthermore most of the coatings used so far can be classified as first generation single layer or classical multilayers, with an individual layer thickness in the micrometer range. Nanoscale superlattice structured coatings have never been explored. CrN/NbN superlattice coatings to protect orthopaedic implants, [82] were deposited in a HIPIMS-enabled Hauzer HTC 1000-4 four-cathode system. Prior to the coating deposition, HIPIMS was used to pre-treat the Co-Cr substrates to produce coatings with enhanced adhesion, [17].

The adhesion strength of various PVD coatings produced by different deposition techniques on femoral components made of ASTM F75 CoCr alloy was investigated. Due to the difficulty of scratch testing upon a curved surface of a real component, a novel experimental set up was developed that allowed an accurate load measurement throughout the test as the diamond indenter traversed over the curved surface. The observed L_C values of various coatings were as follows: CA (Cathodic Arc)-deposited ZrN/CrN: L_{C2} = 19 N, CA-deposited TiNbN: L_{C2} = 38 N and HIPIMS-deposited CrN/NbN: L_{C2} = 50 N, which clearly demonstrated the advantages of the novel HIPMS technology.

Tribological characterisation in dry sliding conditions of uncoated CoCr substrate and CrN/NbN coated by CA and HIPIMS techniques showed unambiguously the advantages of the new approach. HIPIMS-deposited CrN/NbN coatings showed the lowest coefficient of friction of $\mu = 0.49$, compared to $\mu = 0.9$ and $\mu = 0.69$ measured for CA deposited coatings and bare substrate, respectively. Correspondingly the wear coefficient of HIPIMS-deposited

CrN/NbN coatings of $K_C = 4.9 \times 10^{-16}$ m^3 N^{-1} m^{-1} was found to be one order of magnitude lower than that of the CA deposited coatings and thee orders of magnitude lower than that of the bare CoCr substrate.

The deposition process, coating defects and additional roughness generated by coatings are generally considered as a reason for reduction of the fatigue strength of the underlying substrate [83]. This certainly is one of the big challenges for the coating and deposition method selection process for medical articulating implants. Rotating beam fatigue testing in accordance with ASTM F1160 (2014) performed upon CrN/NbN coated and bare ASTM F75 alloy, showed a significant increase in fatigue strength from 349 ± 59 MPa (uncoated) to 539 ± 59 MPa (coated) (t-test $P < 0.001$). This very encouraging positive result is achieved for the first time by a PVD process. It is believed that the fatigue strength increase after coating deposition by HIPIMS can be attributed to two effects. The first effect is the increased compressive stress levels in the substrate surface due to the metal ion implantation during the pre-treatment stage. It is well known that the presence of compressive stress at the surface of the material hinders tensile crack formation and propagation. Second, the low surface roughness and low surface defect density achieved by HIPIMS reduces the number of potential sites for crack initiation. As fatigue properties are known to be dependent largely on geometry, surface finish and load, fatigue tests were carried out on orthopaedic components manufactured from ASTM F75 alloy at physiologically relevant load levels. The coated implants exceeded the expected load requirements and those stipulated in ASTM F1800, showing the suitability of the CrN/NbN coating for use in orthopaedic load bearing applications. This improvement in fatigue life may provide an additional benefit by allowing the development of thinner sectioned more bone-conserving designs of orthopaedic components.

The behaviour of CrN/NbN coated implants has been vigorously evaluated in biological test environments [82]. The metal ion release of the substrate into solution has been examined. ASTM F75 alloy bars representative of the finished orthopaedic products were manufactured, cleaned and sterilised in a manner representative of packaged orthopaedic devices. Two sets of coated (n = 3) and uncoated samples (n = 3) were submerged in 400 g of ultrapure water, and compared to control and spiked samples. These were then incubated at 37 and 70 °C for 28 days, representing physiological and accelerated (more severe) conditions. After initial immersion, a sample of water was taken at the 0 h time point and then after 1, 7, 14 and 28 days a sample (10 g) of liquid was taken and stored for analysis. The analysis was performed with a Perkin Elmer ELAN 6000 Inductively Coupled Plasma-Mass Spectrometry (ICP-MS). The results from ion release tests for Cr, Co and Mo at different time periods taken at low (37 °C) and high (70 °C) temperatures are shown in Figures 27 a-f. The metal ion release studies showed a reduction in Co release at physiological and elevated temperatures over a 28-day period to undetectable levels (<1 ppb) as compared to a peak of 5 ppb for uncoated samples (Figures 27a and 27b). The release of Cr and Mo from the substrate and coated material was below the level of detection, (Figures 27c, d, e, f). Not only is it important to assess the chemical and physical properties of the coating and coated substrates for orthopaedic applications, it is essential that the biological interaction with the coating is assessed. *In vitro* biological testing has been performed in line with the requirements of ISO 10993 in order to assess the safety of the coating in biological environments; cytotoxicity, genotoxicity and sensitisation testing have been performed, all showing no adverse effects. The safety of the coating in biological environments was confirmed through *in vivo* biological testing in sheep.

The HIPIMS technology for production of nanoscale multilayer structured coatings for joint replacement developed at the National HIPIMS Technology Centre in UK has been

transferred to Zimmer Biomet for exploitation and, after successful upscaling, transferred to Ionbond UK for industrial scale production. Photographs of knee implants coated with CrN/NbN HIPIMS at Ionbond UK are shown in Figures 28a, 28b, and 28c.

Acknowledgements:

The authors would like to acknowledge all members of the National HIPIMS Technology Centre at Sheffield Hallam University in UK for their hard work and dedication. Prof. I. Petrov, Prof. P. Barna and Prof. M. Rainforth for the long years of fruitful collaboration. The cooperation with Hauzer Techno Coating and Ionbond from the IHI Group over the years is deeply acknowledged.

References:

[1] L. Johansson, Röntgenographische Bestimmung der Atomanordnung in den Mischkristallreihen AuCu und PdCu, Annalen der Physik. 78 (1925) 439. doi:10.1002/andp.19253832104.

[2] J. S. Koehler, Attempt to Design a Strong Solid, Phys. Rev. B. 2 (1970) 547-551. https://doi.org/10.1103/PhysRevB.2.547

[3]. N. J. Petch, The Cleavage Strength of Polycrystals, J. Iron Steel Inst. 174 (1953) 25-28.

[4]. R. C. Cammarata, T.E. Schlesinger, C. Kim, S.B. Quadri, A.S. Edelstein, Nanoindentation study of the mechanical properties of copper-nickel multilayer thin film, Appl. Phys. Lett. 56 (1990) 1862-1864. https://doi.org/10.1063/1.103070

[5]. B. M. Clemens, H. Kung, S. A. Barnett, Interaction of dislocations with incoherent interfaces in nanoscale FCC–BCC metallic bi-layers, Mater. Res. Soc. Bull. 24 (1999) 20.

[6] X. Chu and S. Barnett. Model of superlattice yield stress and hardness enhancement, J. Appl. Physics. 77 (1995) 4403-4411. https://doi.org/10.1063/1.359467

[7] U. Helmersson, S. Todorova, , S. Barnett, J.-E.Sundgren, L. Markert, , and J. E. Greene, (1987). Growth of single-crystal TiN/VN strained-layer superlattices with extremely high mechanical hardness, J. Appl. Phys. 62 (1987) 481-484. https://doi.org/10.1063/1.339770.

[8]. M Setoyama, A. Nakayama, M. Tanaka, N. Katagawa, and T. Nomura, Formation of cubic-A1N in TiN/A1N superlattice, Surf. Coat. Tech. 86-87 (1996) 225-230. https://doi.org/10.1016/S0257-8972(96)03033-2.

[9] W.-D. Münz, D. Schulze, F.J.M. Hauzer, A new method for hard coatings: ABS^{TM} (arc bond sputtering), Surf. Coat.Tech. 50 (1992) 169. https://doi.org/10.1016/0257-8972(92)90058-I

[10]. W.-D. Münz, D. B. Lewis, P. Eh. Hovsepian, C. Schönjahn, A. Ehiasarian, I. J. Smith, Industrial scale manufactured superlattice structured hard PVD coatings, Surf. Eng. 17 (1) (2001) 15-27. https://doi.org/10.1179/026708401101517557.

[11]. P. Eh. Hovsepian, W.-D. Münz, "Synthesis, Structure and Applications of Nanoscale Multilayer/Superlattice Structured PVD Coatings" in Nanostructured Coatings, Edited by A. Cavaleiro and J. Th. M. De Hosson, Springer/Kluwer, 2005, 555-644.

[12]. P.Yashar, S.A. Barnett, J.Rechner, W.D. Sproul, Structure and mechanical properties of polycrystalline CrN/TiN superlattices, J. Vac. Sci. Technol. A 16 (5) (1998) 2913. https://doi.org/10.1116/1.581439

[13]. P. Eh. Hovsepian, Influence of the parameters of the metal ion etching on the structure and the adhesion of TiN coatings deposited by the Cathodic Arc Evaporation in vacuum, Archives of Metallurgy, Polish Academy of Sci. 33(4) (1988) 577-582.

[14] C. Schönjahn, L. A. Donohue, D. B. Lewis, W.-D. Münz, R. D. Twesten, and I. Petrov, Enhanced adhesion through local epitaxy of transition-metal nitride coatings on ferritic steel promoted by metal ion etching in a combined cathodic arc/unbalanced magnetron deposition system, *J. Vac. Sci. Technol.* **A 18(4)** (2000) 1718-1723. https://doi.org/10.1116/1.582414

[15] J.M. Lafferty, Vacuum Arcs- Theory and Applications, Wiley, New York, 1980.

[16] H. W. Wang, M.M Stack, S.B. Lyon, P. Hovsepian, W.-D. Münz, The corrosion behaviour of macroparticle defects in arc bond-sputtered CrN/NbN superlattice coatings, Surf Coat Tech.126 (2000) 279-287. https://doi.org/10.1016/S0257-8972(00)00554-5

[17]. A. P. Ehiasarian, P. Eh. Hovsepian, W.-D. Münz, "A Combined Process Comprising Magnetic Field-Assisted, High-Power, Pulsed Cathode Sputtering and an Unbalanced Magnetron"Granted: US 10718435, 2005, EP 1 260 603 A2, DE 10124749, 21.05. 2001.

[18] A. P. Ehiasarian, Y. A. Gonzalvo, T. D. Whitmore, Time-Resolved Ionisation Studies of the High Power Impulse Magnetron Discharge in Mixed Argon and Nitrogen Atmosphere, Plasma Process. Polym. 4 (2007) S309–S313. https://doi.org/10.1002/ppap.200730806.

[19] A. P. Ehiasarian, J. G. Wen, and I. Petrov, Interface microstructure engineering by high power impulse magnetron sputtering for enhanced adhesion, J. Appl. Phys. 101 (2007) 054301. https://doi.org/10.1063/1.2697052

[20]. A. P. Ehiasarian, P. Eh. Hovsepian, L. Hultman, U. Helmersson, Comparison of microstructure and mechanical properties of chromium nitride-based coatings deposited by high power impulse magnetron sputtering and by the combined steered cathodic arc/unbalanced magnetron technique, Thin Solid Films, 457 (2) (2004) 270-277. https://doi.org/10.1016/j.tsf.2003.11.113

[21] A. P. Ehiasarian, A. Vetushka, Y. Aranda Gonzalvo, G. Safran, L. Szekely, P. B. Barna, Influence of high power impulse magnetron sputtering plasma ionization on the microstructure of TiN thin films, J. Appl. Physics 109 (2011) 104314. https://doi.org/10.1063/1.3579443

[22] D. McIntyre, J. E. Greene, G. Håkansson, J.-E. Sundgren, and W.-D.Münz, Oxidation of metastable single–phase polycrystalline Ti0.5Al0.5 N films: kinetics and mechanisms, J. Appl. *Phys.* **67** (1990) 1542-1553. https://doi.org/10.1063/1.345664

[23] L.A. Donohue, I.J. Smith, W.-D.Münz, I. Petrov, and J.E. Greene, Microstructure and oxidation-resistance of $Ti_{1-x-y-z}Al_xCr_yY_zN$ layers grown by combined steered-arc/unbalanced-magnetron-sputter deposition, Surf Coat Tech. 94/95 (1997) 226-231. https://doi.org/10.1016/S0257-8972(97)00249-1.

[24] C. Leyens, R. Braun, M. Fröhlich and P.Eh. Hovsepian, Recent progress in the coating protection of Gamma Titanium –Aluminides, JOM, 58 (1) (2006) 17-21. https://doi.org/10.1007/s11837-006-0062-4

[25] I. Petrov, P. Losbichler, D. Bergstrom, J.E. Greene, W.-D. Münz, T. Hurkmans, T. Trinh, Ion-assisted growth of $Ti_{1-x}Al_xN/Ti_{1-y}Nb_yN$ multilayers by combined cathodic-arc/magnetron-sputter deposition, Thin Solid Films 302 (1997) 179-192. https://doi.org/10.1016/S0040-6090(96)09524-7.

[26]. P. Eh. Hovsepian, A.P. Ehiasarian, R. Braun, J. Walker, H. Du, Novel CrAlYN/CrN nanoscale multilayer PVD coatings produced by the combined High Power Impulse Magnetron Sputtering/Unbalanced Magnetron Sputtering technique for environmental protection of γ-TiAl alloys. Surf. Coat. Tech. 204 (2010) 2702-2708. https://doi:10.1016/j.surfcoat.2010.02.021

[27] P. Hovseapian, A. P. Ehiasarian, R. Tietema, C. Strondel, A method for the manufacture of a hard metal coating on a substrate, UK Patent GB 2450950, 19.05. 2010, priority date 02. 01. 2008.

[28] P. Eh. Hovsepian, A. P. Ehiasarian, Y. P. Purandare, P. Mayr, K. G. Abstoss, M. Mosquera- Faijoo, W. Schulz, A. Kranzmann, M. I. Lasanta, J. Trulillo, Novel HIPIMS deposited nanostructured CrN/NbN coatings for environmental protection of steam turbine components, J. Alloy. Compd. 746 (2018) 583-593 https://doi.org/10.1016/j.jallcom.2018.02.312

[29] R. Braun, U.Schulz, C. Leyens, P. E. Hovsepian, A. P.Ehiasarian, Oxidation and fatigue behaviour of γ-TiAl coated with HIPIMS CrAlYN/CrN nanoscale multilayer coatings and EB-PVD thermal barrier coatings, Int. J. Mater. Res. 101 (5) (2010) 648-656. https://doi.org/10.3139/146.110323

[30] A. Skopp, M. Woydt, Ceramic and Ceramic Composite Materials with Improved Friction and Wear Properties**,** Tribol. Trans. 38 (2) (1995) 233-242. https://doi.org/10.1080/10402009508983400

[31]. W.D. Münz, D. Hofmann and K. Harting, A high rate sputtering process for the formation of hard friction-reducing TiN coatings on tools, Thin Solid Films. 96 (1982) 79-86. https://doi.org/10.1016/0040-6090(82)90215-2.

[32] U. König, Deposition and properties of multicomponent hard coatings, Surf Coat Tech. 33 (1987) 91-103. https://doi.org/10.1016/0257-8972(87)90180-0.

[33] U. König, W. Shulz. Untersuchungsber. UB2016,1984, (Krupp Widia GmbH, Postfach 102161, D-4300, Essen1).

[34] K. Noguchi, N. Kitagawa, H. Ohara, and H. Animoto, High speed drilling with coated carbide drills. Proc. 1st French- German Conf. High Speed Machining, University of Metz , France. 1997, pp 407-413.

[35] C.P. Constable, J. Yarwood, P. Hovsepian, L. A. Donohue, D. B. Lewis, W.-D. Münz, Structural determination of wear debris generated from sliding wear tests on ceramic coatings using Raman microscopy, J. Vac. Sci. Technol. A 18(4) (2000) 1681. https://doi.org/10.1116/1.582407

[36] P. H. Mayrhofer, P.Eh. Hovsepian, W.-D. Münz, C. Mitterer, Calorimetric evidence for frictional self-adaptation of TiAlN/VN superlattice coatings, Surf Coat Tech. 177 (2004) 341-347. https://doi.org/10.1016/j.surfcoat.2003.09.024.

[37] O. Knotek, T. Leyendecker, F. Jungblut. On the properties of physical deposited Ti-Al-V-N coatings. Thin Solid Films, 153 (1987) 83-90. https://doi.org/10.1016/0040-6090(87)90172-6.

[38] R. Hann, M. Bartosik, R. Soler, C. Kirchlechner, G. Dehm, P.H. Mayerhofer, Superlattice effect for enhanced fracture toughness of hard coatings. Scripta Materialia 124 (2016) 67-70. https://doi.org/10.1016/j.scriptamat.2016.06.030.

[39] P.Eh.Hovsepian, D.B.Lewis, , and W.-D. Münz, Recent Progress in Large Scale Manufacturing of Multilayer/Superlattice Hard Coatings, Surf. Coat. Technol. 133 (2000)166-175. https://doi.org/10.1016/S0257-8972(00)00959-2.

[40] W.-D.Münz, L.A.Donohue, and P. Eh. Hovsepian, Properties of various large –scale fabricated TiAlN- and CrN- based superlattice coatings grown by combined cathodic arc-unbalanced magnetron sputter deposition. Surf. Coat. Technol. 125 (2000) 269-277. https://doi.org/10.1016/S0257-8972(99)00572-1.

[41] Q. Luo, Z. Zhou, W.M. Rainforth, P. Eh. Hovsepian, TEM-EELS study of low- friction superlattice TiAlN/VN coating: the wear mechanism, Tribol. Lett. 24(2) (2006) 171-178. https://doi.org/10.1007/s11249-006-9160-2.

[42] S. Barnett, A. Madan: Superhard Superlattices, Phys. World, 11 (1998) 45-48. https://doi.org/10.1088/2058-7058/11/1/34.

[43] P. Eh. Hovsepian, Y. N. Kok, A. P. Ehiasarian, R. Haasch, J.-G. Wen, I. Petrov, Phase separation and formation of the self-organised nanostructure in C/Cr coatings in conditions of high ion irradiation, Surf Coat Tech. 200 (2005) 1572-1579. https://doi.org/10.1016/j.surfcoat.2005.08.095.

[44] P. Eh. Hovsepian, A.P. Ehiasarian, U. Rataysaki, CrAlYCN/CrCN Nanoscale multilayer PVD coatings deposited by the combined High Power Impulse Magnetron Sputtering/Unbalanced Magnetron Sputtering (HIPIMS/UBM) technology, Surf Coat Tech. 203 (2009) 1237–1243. https://doi.org/10.1016/j.surfcoat.2008.10.033.

[45] Q. Luo, C. Schimpf, A. P. Ehiasarian, P. Eh. Hovsepian, Structure and Wear Mechanisms of Nano-Structured TiAlCN/VCN Multilayer coatings, Plasma Process. Polym. , 4 (2007) S916–S920. https://onlinelibrary.wiley.com/doi/pdf/10.1002/ppap.200732205.

[46] P. Eh. Hovsepian, A. P. Ehiasarian, I. Petrov, C. Schimpf, TiAlCN/VCN Nanoscale Multilayer PVD Coatings Deposited by the Combined High Power Impulse Magnetron Sputtering/ Unbalanced Magnetron Sputtering Technology Dedicated to Machining of Al and Ti Alloys. Surface Engineering 26 (2010) 610-614. DOI 10.1179/026708408X336337.

[47] European project "ALTICUT" GRD1-2001-40514, Final Report.

[48] P. Eh. Hovsepian, A. P. Ehiasarian , A. Deeming , C. Schimpf. VMeCN Based Nanoscale Multilayer PVD Coatings Deposited by the Combined High Power Impulse Magnetron Sputtering/Unbalanced Magnetron Sputtering Technology, *Plasma Process. Polym.* 4 (2007) S897-S901. https://doi.org/10.1002/ppap.200732201

[49] P. Eh. Hovsepian, A. P. Ehiasarian, PVD Coated Substrate, Patents US 8173248B2, EP 1 874 981 B1, DE602006004862D1, WO2006114610A1, GB2425780B.

[50] A. H. S Jones, D. Camino, D. G. Teer, J. Jiang, Novel high wear resistant diamond-like carbon coatings deposited by magnetron sputtering of carbon targets, Proc. Inst. Mech. Eng. Tribol. 212 (1998) 301-306. DOI: 10.1243/13506509815442119 .

[51] M. Stueber, U. Albers, H. Leiste, S. Ulrich, H. Holleck, P.B. Barna , A. Kovacs, P.Eh. Hovsepian, I. Gee, Multifunctional nanolaminated PVD coatings in the system Ti-Al-N-C by combination of metastable fcc phases and nanocomposite microstructures. Surf Coat Tech. 200 (2006) 6162-6171. https://www.sciencedirect.com/science/article/pii/S0257897205012041

[52] Uglova,V.M. Anishchik, Y.Pauleau, A.K. Kuleshov, F.Thiery, J. Pelletier, S.N. Dub, and D.P. Rusalsky, Relations between deposition conditions, microstructure and mechanical properties of amorphous carbon-metal films, *Vacuum* **70 (2003)** 181-185. https://doi.org/10.1016/S0042-207X(02)00639-5.

[53] J. Neidhart, A. Czigany, I.F.Brunell, and L. Hultman, (2003), Growth of fullerene-like carbon nitride thin solid films by reactive magnetron sputtering; Role of low-energy ion irradiation in determining microstructure and mechanical properties, J. Appl. Phys. **93** (2003) 3002-3015. https://doi.org/10.1063/1.1538316

[54]. I. Petrov, P.B. Barna, L. Hultman, J.E. Greene, Microstructural evolution during film growth, J. Vac. Sci. Technol. A 21 (5) (2003) 117. https://doi.org/10.1116/1.1601610

[55]. S. Veprek, R.S. Reiprich, A concept for the design of novel superhard coatings, Thin Solid Films 268 (1995) 64-71. https://doi.org/10.1016/0040-6090(95)06695-0

[56] B. Chapman. Glow Discharge Processes: Sputtering and Plasma Etching, John Wiley & Sons Inc. New York, 1980.

[57] P.Eh. Hovsepian, Y.N. Kok, A.P. Ehiasarian, A. Erdemir, I. Petrov, W.-D. Münz, Structure and Tribological Properties of Nanoscale Multilayer C/Cr Coatings Deposited by the Combined Steered Cathodic Arc/ Unbalanced Magnetron Sputtering Technique, Thin Solid Films, 447-448 (2004) 7-13. https://doi.org/10.1016/j.tsf.2003.09.009.

[58] Y.N. Kok , J.-G. Wen , I. Petrov, P. Eh. Hovsepian, Influence of ion bombardment on structure and tribological performance of nanoscale multilayer C/Cr PVD coatings. Surface Engineering, 22 (2) (2006) 92-98 . https://doi.org/10.1179/174329406X98377

[59] M. Priest, C.M. Taylor, Automobile engine tribology – approaching the surface, Wear 241 (2) (2000) 193–203. https://doi.org/10.1016/S0043-1648(00)00375-6.

[60] Y. Liu, A. Erdemir, E.I. Meletis, An investigation of the relationship between graphitization and frictional behaviour of DLC coatings, Surf Coat Tech. 86–87 (1996) 564–568. https://doi.org/10.1016/S0257-8972(96)03057-5.

[61] H. Ronkainen, K. Holmberg, Environmental and thermal effects on thetribological performance of DLC coatings, in: A.E.C. Donnet (Ed.), Tribology of Diamond-Like Carbon Films, Springer, 2008, pp. 155–196.

[62] Y. Yamamoto, S. Gondo, Friction and wear characteristics of molybdenum dithiocarbamate and molybdenum dithiophosphate, Tribol. Trans. 32(2) (1989) 251–257. https://doi.org/10.1080/10402008908981886

[63] S. Miyake, T. Saito, Y. Yasuda, Y. Okamoto, M. Kano, Improvement of boundarylubrication properties of diamond-like carbon (DLC) films due to metal addition, Tribol. Int. 37 (2004) 751–761. https://doi.org/10.1016/j.triboint.2004.01.014.

[64] M.d. Barros'Bouchet, J. Martin, T. Le-Mogne, B. Vacher, Boundary lubrication mechanisms of carbon coatings by MoDTC and ZDDP additives, Tribol. Int. 38 (2005) 257–264. https://doi.org/10.1016/j.triboint.2004.08.009

[65] P. Eh. Hovsepian, P. Mandal, A. P. Ehiasarian, G. Safran, R. Tietema, D. Doerwald, Friction and wear behaviour of Mo-W doped carbon -based coating during boundary lubricated sliding, Appl Surf Sci. 366 (2016) 260-274. https://doi.org/10.1016/j.apsusc.2016.01.007

[66] J. Sharp, I. Castillo Muller, P. Mandal, A. Abbas, G. West, W. M. Rainforth, A. Ehiasarian, P. Eh. Hovsepian, Characterisation of a High-Power Impulse Magnetron Sputtered C/Mo/W Wear Resistant Coating by Transmission Electron Microscopy, J Phys. Conf. Ser. 644 (2015) 012011. http://iopscience.iop.org/1742-6596/644/1/012011.

[67] P. Mandal, A. P. Ehiasarian, P. Eh. Hovsepian, Isothermal and dynamic oxidation behaviour of Mo-W doped carbon-based coating, Appl. Surf. Sci. 353 (2015)1291-130. https://doi.org/10.1016/j.apsusc.2015.07.057

[68] P. Eh. Hovsepian, D. Doerwald, R. Tietema, A.P. Ehiasarian. Me-doped C coating to operate in boundary lubrication conditions where the metal to C ratio does not exceed 1:4. European Patent 2 963 145. Priority claimed: 30.04.2014. EP/30.06.2014/EPA 14175063.

[69] P. Eh. Hovsepian, D. B. Lewis, W.-D. Münz, A. Rouzaud, P. Juliet, Chromium nitride/niobium nitride superlattice coatings deposited by the combined cathodic-arc/unbalanced magnetron technique, Surf Coat Tech. 116-119 (1999) 727-734. https://doi.org/10.1016/S0257-8972(99)00182-6.

[70] P. Eh. Hovsepian, D. B. Lewis, W.-D. Münz, S. B. Lyon, M. Tomlinson. Combined cathodic arc/unbalanced magnetron grown CrN/NbN superlattice coatings for corrosion resistant applications, Surf Coat Tech. 120-121 (1999) 535-541. https://doi.org/10.1016/S0257-8972(99)00439-9.

[71] P. Eh. Hovsepian , Q.Luo , D. B. Lewis, A. Farinotti. Corrosion resistance of CrN/NbN superlattice coatings grown by various physical vapour deposition techniques. Thin Solid Films. 488 (2005) 1-8. https://doi.org/10.1016/j.tsf.2005.03.016

72] C. Reinhard, A. P. Ehiasarian, P. Eh. Hovsepian. CrN/NbN superlattice coatings with enhanced corrosion resistance achieved by high power impulse magnetron sputtering

interface pre-treatment., Thin Solid Films 515 (2007) 3685-3692. https://doi.org/10.1016/j.tsf.2006.11.014.

[73] Y. P. Purandare, A. P. Ehiasarian, and P. Eh. Hovsepian. Deposition of nanoscale multilayer CrN/NbN physical vapour deposition coatings by high power impulse magnetron sputtering. J. Vac. Sci. Technol. A 26 (2008) 288-296. https://doi.org/10.1116/1.2839855

[74] A.A. Sugumaran, Y. Purandare, A. P. Ehiasarian, P. Eh. Hovsepian, Corrosion behaviour of post-deposition polished droplets-embedded arc evaporated and droplets-free HIPIMS/DCMS coatings, Corrosion, 73 (6) (2017) 685-693. https://doi.org/10.5006/2064.

[75] P. Eh. Hovsepian, W.-D. Münz, Bright- Euram Project: "**NEWCHROME":** "Environmentally Friendly and Hardness Enhanced PVD CrN/TaN Superlattice Coatings as a Novel Alternative to Plated Hard Chrome";Brite /Euram BE96-3305, Final Report, 29.02 2000.

[76] P. Eh. Hovsepian, W.-D. Münz , B.Schlömer, G. Gregory, and I. J. Smith, (2001). PVD CrN/NbN superlattice coatings to protect components used in textile industry. Proceedings of 44th, Annual Conference of Soc. of Vacuum Coaters SVC, April 2001, Philadelphia, USA, pp.72-77.

[77] P. Eh. Hovsepian, W.-D. Münz, A. Medlock, G. Gregory, Combined Cathodic Arc/Unbalanced Magnetron Grown CrN/NbN Superlattice Coatings for Applications in the Cutlery Industry, Surf. Coat. Technol. 133 (2000) 508-516. https://doi.org/10.1016/S0257-8972(00)00921-X.

[78] P. Eh. Hovsepian, A. P. Ehiasarian, Y. P. Purandare, B. Biswas, F.J. Perez, M.I.Lasanta, M. T. de Miguel, A. Illana, M. Juez-Lorenzo, R. Muelas, A. Agüero. Performance of HIPIMS deposited CrN/NbN nanostructured coatings exposed to 650^{o}C in pure steam environment, Mater. Chem. Phys. 179 (2016) 110-119. https://doi.org/10.1016/j.matchemphys.2016.05.017

[79] P. Eh. Hovsepian, A. P. Ehiasarian, Y. P. Purandare, P. Mayr, K. G. Abstoss, M. Mosquera- Faijoo, W. Schulz, A. Kranzmann, M. I. Lasanta, J. Trulillo, Novel HIPIMS deposited nanostructured CrN/NbN coatings for environmental protection of steam turbine components. J. Alloys Compd. 746 (2018) 583-593. https://doi.org/10.1016/j.jallcom.2018.02.312

[80] A. Aguero, R. M. Gamo, M. J. Lorenzo, P. Hovsepian, Y. Purandare, A. Ehiasarian, Long-term behaviour of Nb and Cr nitrides nanostructured coatings under steam at 650 °C mechanistic considerations. J. Alloys Compd. 739 (2018) 549-558. https://doi.org/10.1016/j.jallcom.2017.12.288

[81] Okazaki Y, Gotoh E., Comparison of metal release from various metallic biomaterials in vitro, Biomaterials. 26 (1) (2005)11–21. https://doi.org/10.1016/j.biomaterials.2004.02.005

[82] P. Eh. Hovsepian, A. P. Ehiasarian, Y. Purandare, A. Sugumaran, T. Marriott, I. Khan. J. Development of superlattice CrN/NbN coatings for joint replacements deposited by high power impulse magnetron sputtering, J. Mater. Sci. Mater. Med. 27 (2016) 147. https://doi.org/10.1007/s10856-016-5751-0

[83] M.Y.P. Costa, M.L.R. Venditti, M.O.H. Cioffi, H.J.C. Voorwald, V.A. Guimarães, R. Ruas. Fatigue behavior of PVD coated Ti–6Al–4V alloy, Int J Fatigue. 33 (6) (2011) 759–765. https://doi.org/10.1016/j.ijfatigue.2010.11.007

Figures

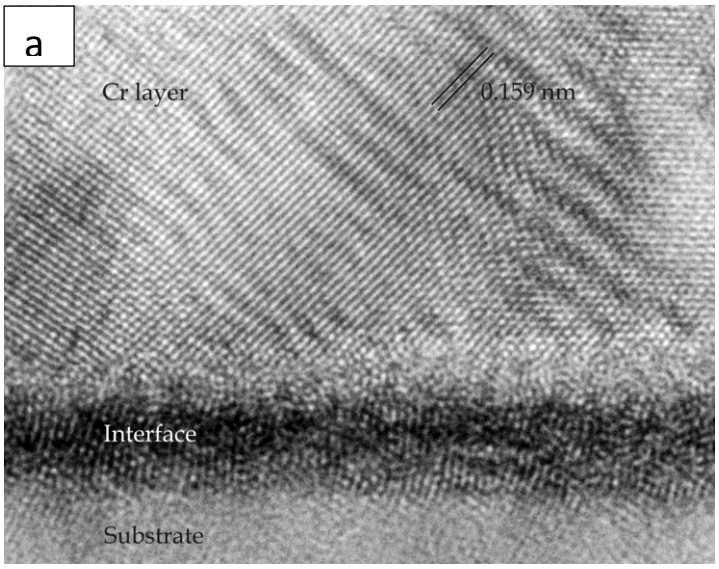

Figure 1: a) High resolution TEM image of the Cr coating-substrate interface pre-treated by Ar ion bombardment, amorphised interface, (*Image, courtesy of Jeff Th.M. De Hosson, Dept. Appl. Phys. Mater. Sci. Centre, University of Groningen, The Netherlands*),

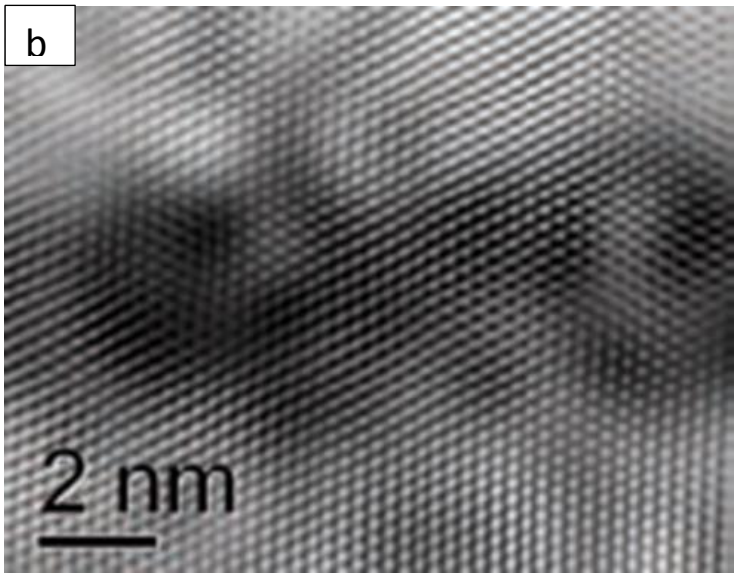

Figure 1: b) Atomic Resolution TEM image of CrN coating-substrate interface pre-treated by HIPIMS showing the highly preserved interface crystallinity, (*Image, courtesy of EC, INNOVATIAL Project, NMP3-CT-2005-515844*).

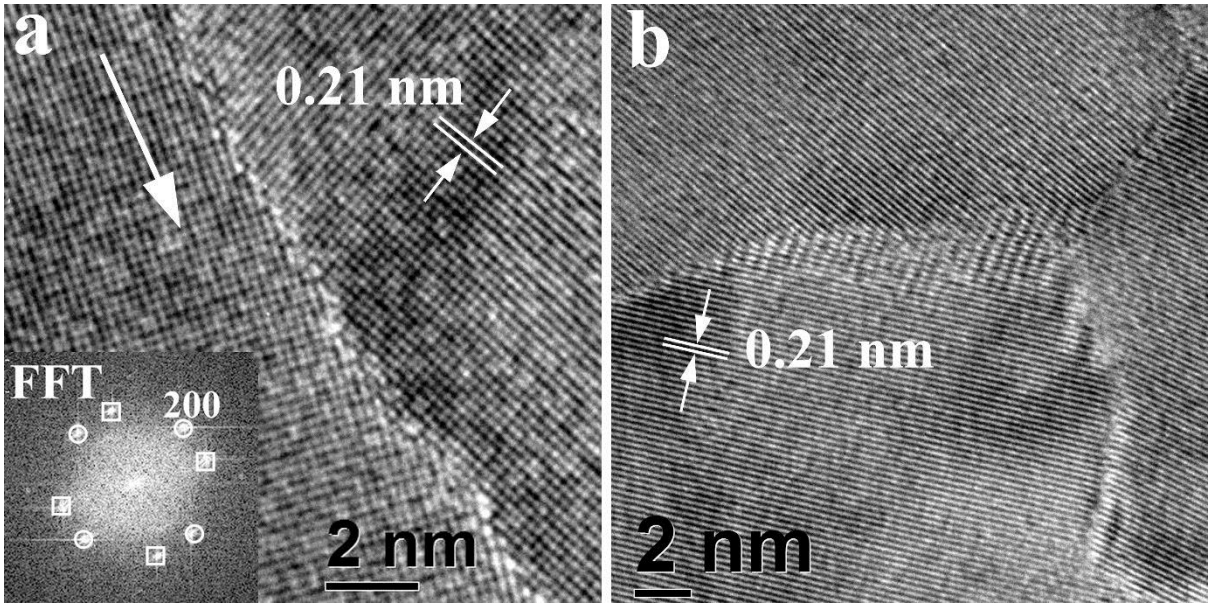

Figure 2: High resolution cross sectional (a) and plane-view (b) HRTEM micrographs of the film. The arrow in (a) shows the growth direction of the film.

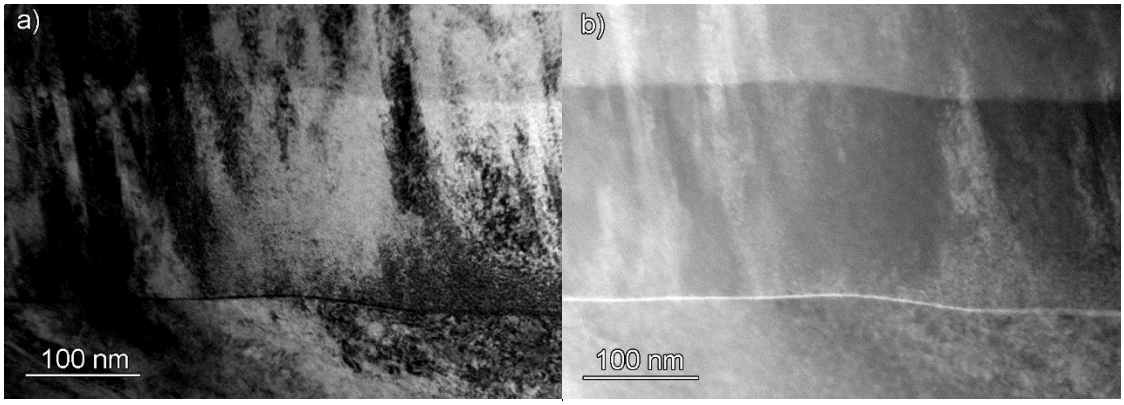

Figure 3. (a) Bright field and (b) Z-contrast STEM images of the substrate/coating interface region, reproduced from [26].

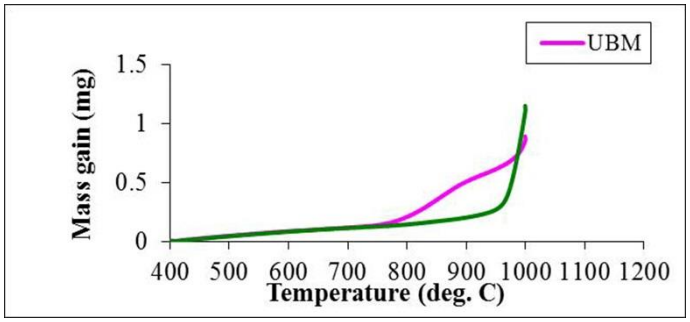

Figure 4. Mass gain vs. temperature of γ-TiAl specimens coated with CrAlYN/CrN using UBM and HIPIMS techniques.

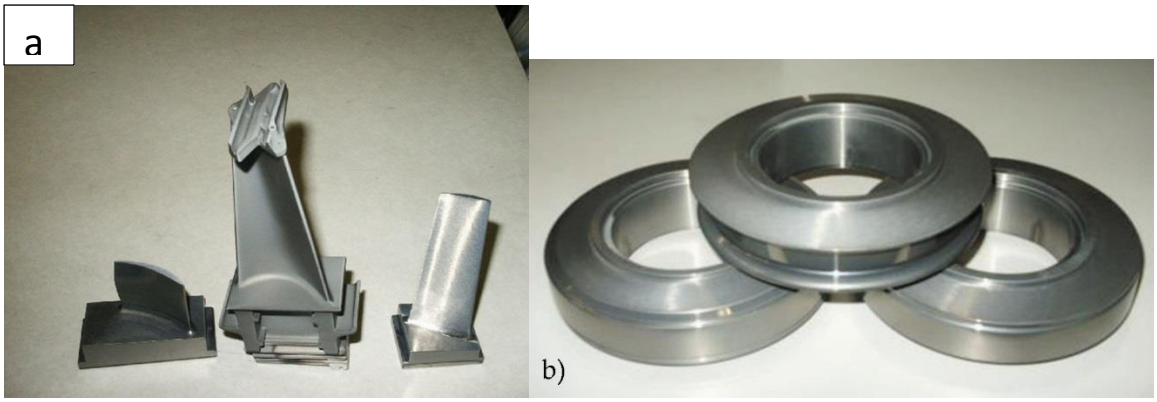

Figure 5. CrAlYN/CrN coated: a) turbine blades, b) cemented carbide dies for hot rolling of steel at 950°C.

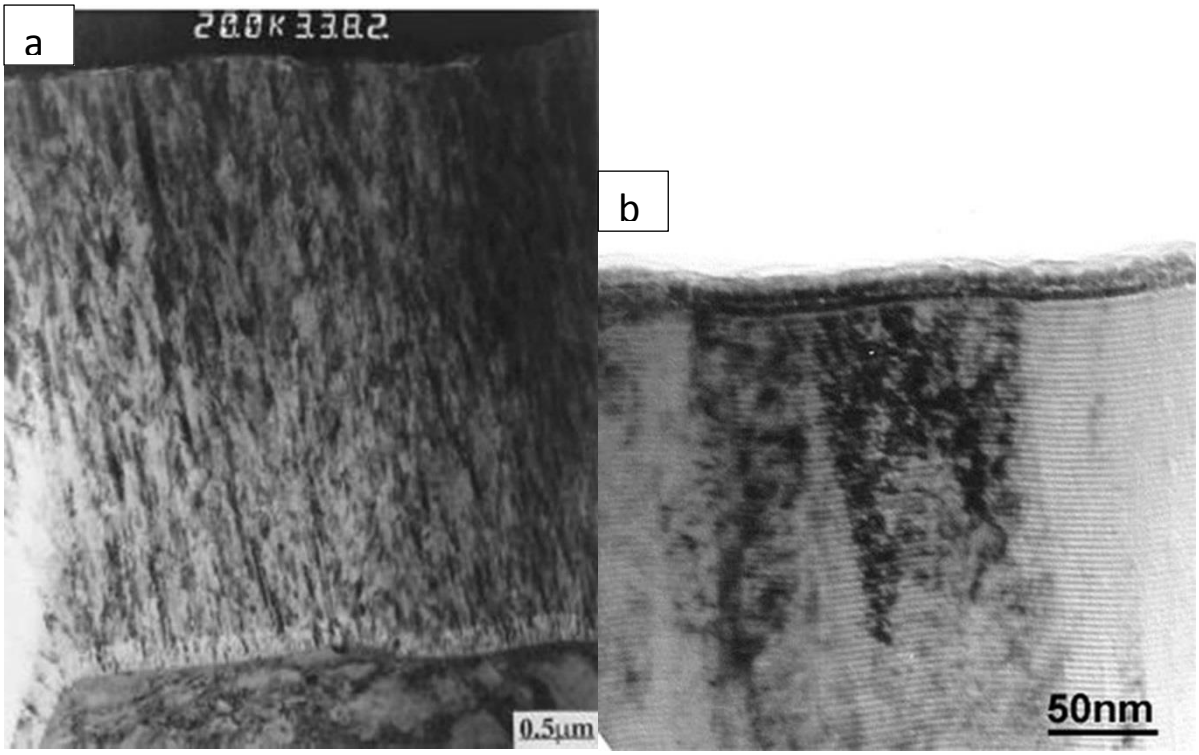

Figure 6. Low magnification, a) and high magnification, b), bright-field XTEM images of TiAlN/VN superlattice coating.

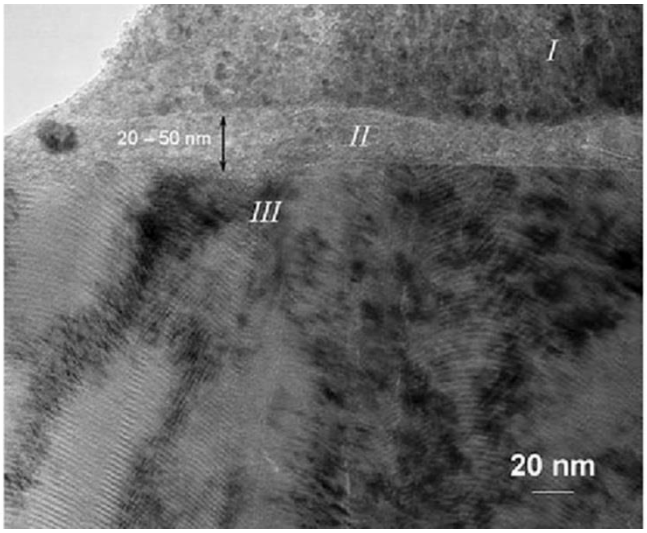

Figure 7. Cross-sectional TEM bright field image of the TiAlN/VN superlattice coating from the wear track region after pin-on-disc test showing the tribo-film formation, where: zone I is copper re-deposit formed during the TEM sample preparation, (ion -beam thinning), zone II shows the structure of the 20-50 nm thick tribo-film and zone III shows the structure of the superalattice coating reproduced from [41].

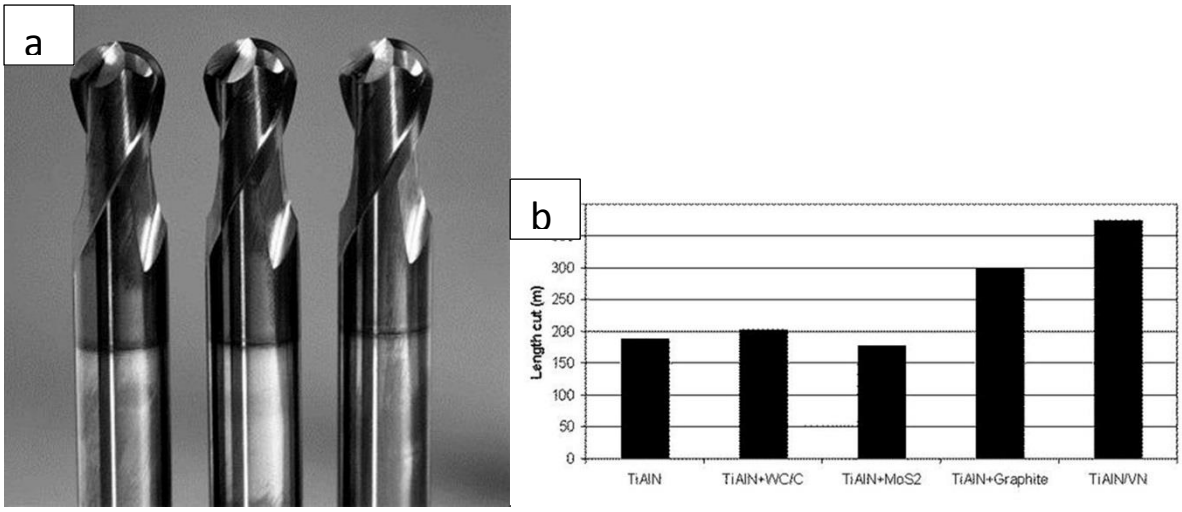

Figure 8: a) TiAlN/VN coated 8 mm two- flute ball nosedcutters(Whisper Mill, Hydra Tools, Sheffield, UK), b) Life time of various PVD coatings under dry-milling conditions of Inconel 718 alloy, (*Source: D.K. Aspinwall, R.C. Dewes, E.-G. Ng, C. Sage, S.L. Soo, University of Birmingham, Rolls-Royce plc, Filton*).

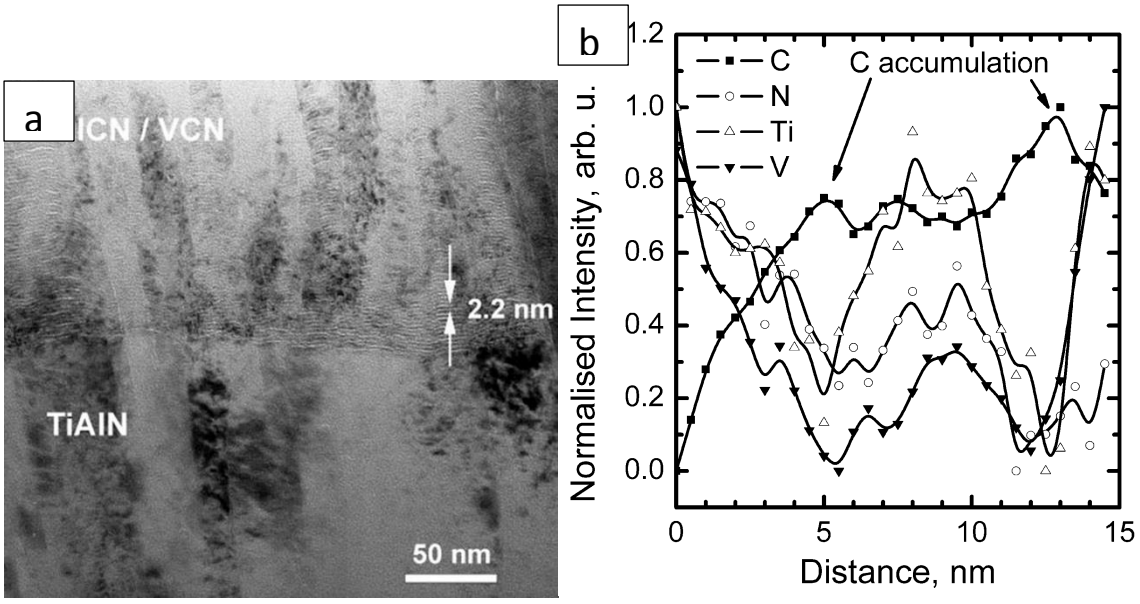

Figure 9: a) High magnification bright field XTEM image of TiAlCN/VCN, (reproduced from [48]) and b) Qualitative STEM–EELS analysis of segregated layered phase (carbon is seen to accumulate in layers where Ti, V and N content are depleted, (reproduced from [46]).

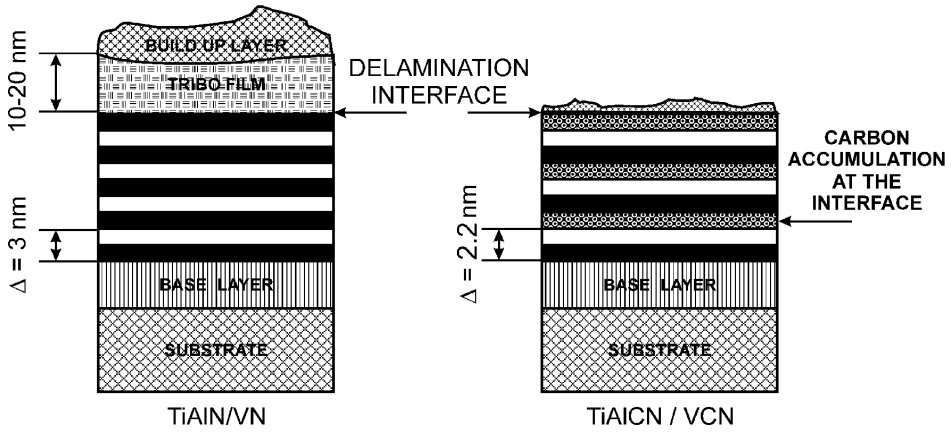

Figure 10. Schematic illustration the wear mechanisms of carbon free and carbon containing coatings, (reproduced from [46]).

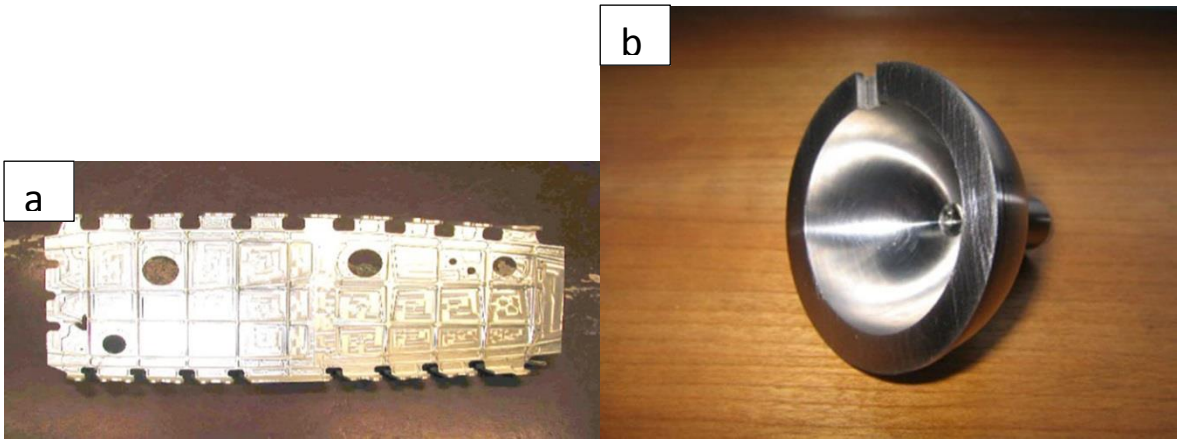

Figure 11 a) Wingbox rib of an A380 airplane and b) TiAl6V4 orthopaedic implant.

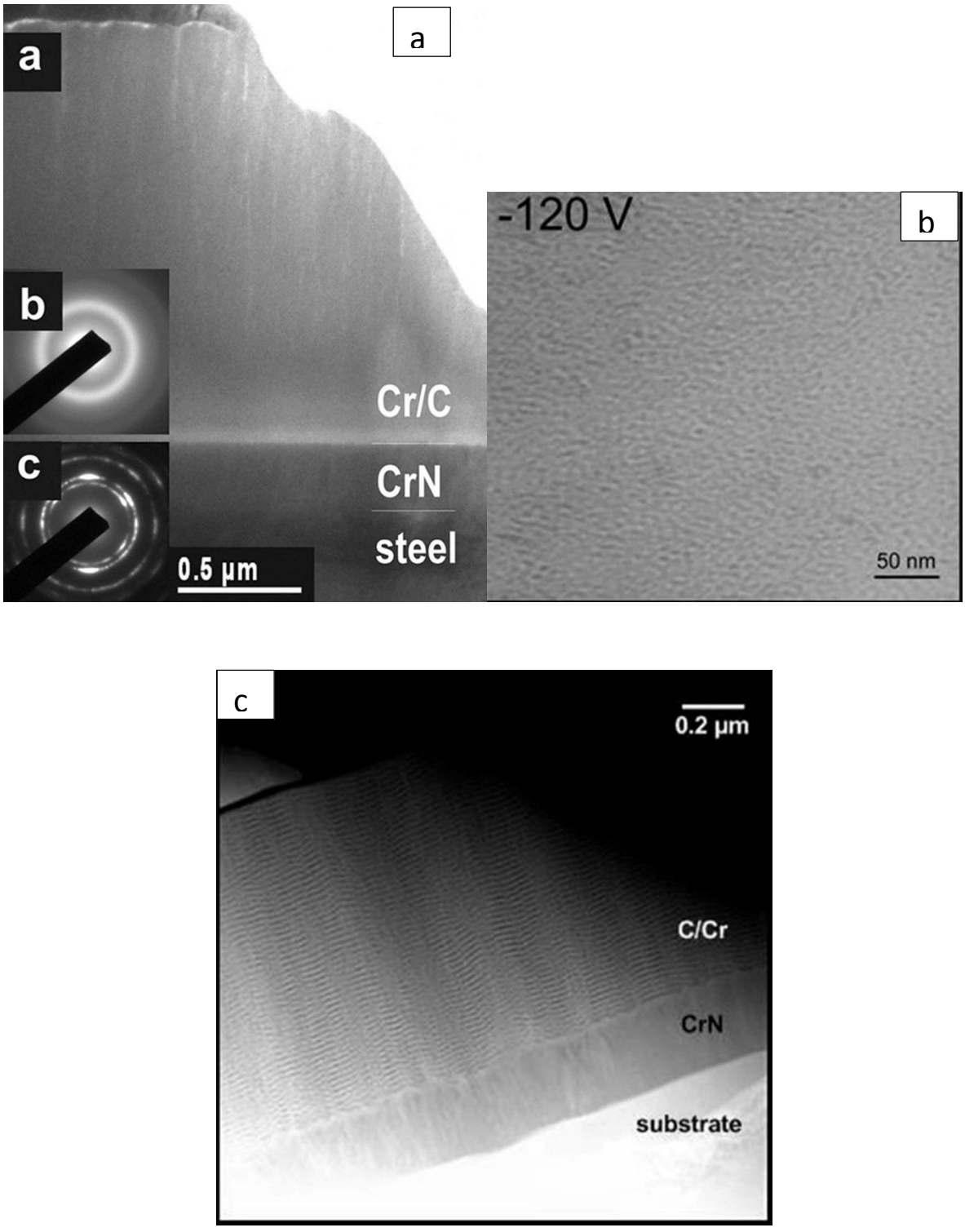

Figure 12. HRTEM image of C/Cr film deposited at: a) U_b = -65V, b) U_b = -120V and c) U_b = -350V.

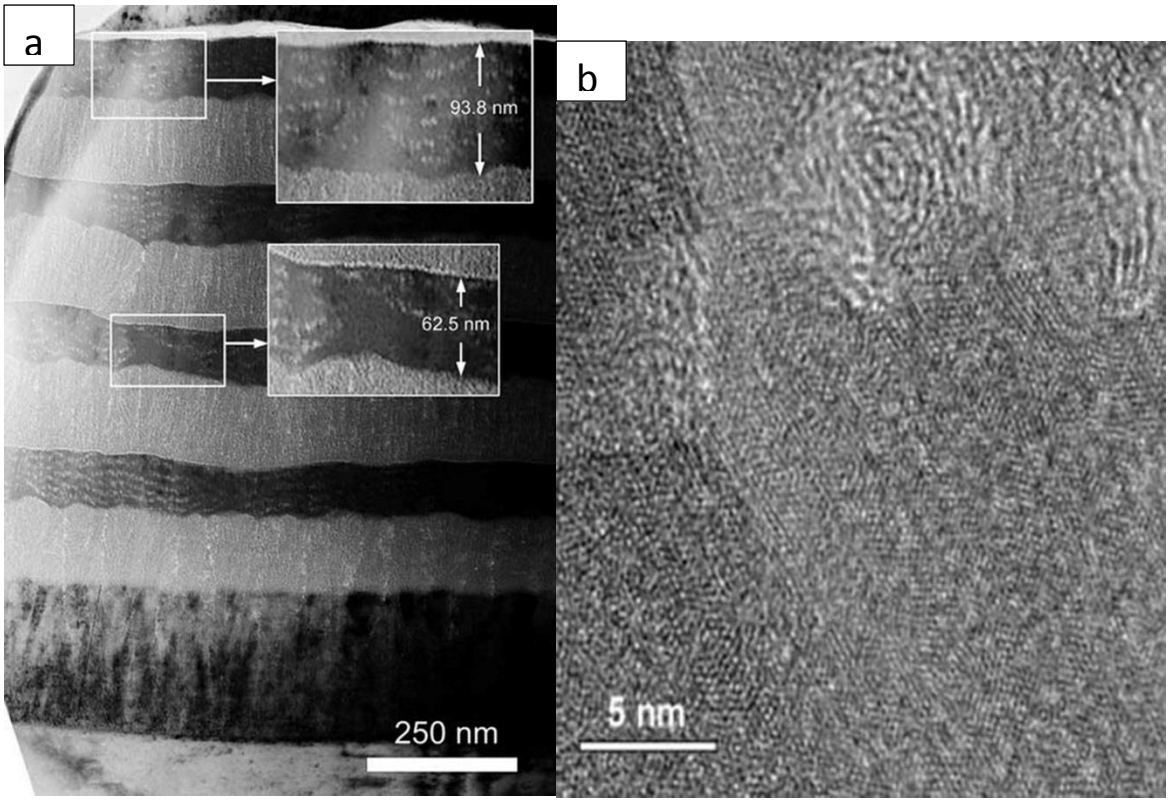

Figure 13. a) BF XTEM image of the overall structure of the coating deposited at bias voltage altered from low (U_b = - 75 V) to high (U_b = - 350 V) in four cycles, (reproduced from [43]) and b) higher magnification image of the C-rich clusters.

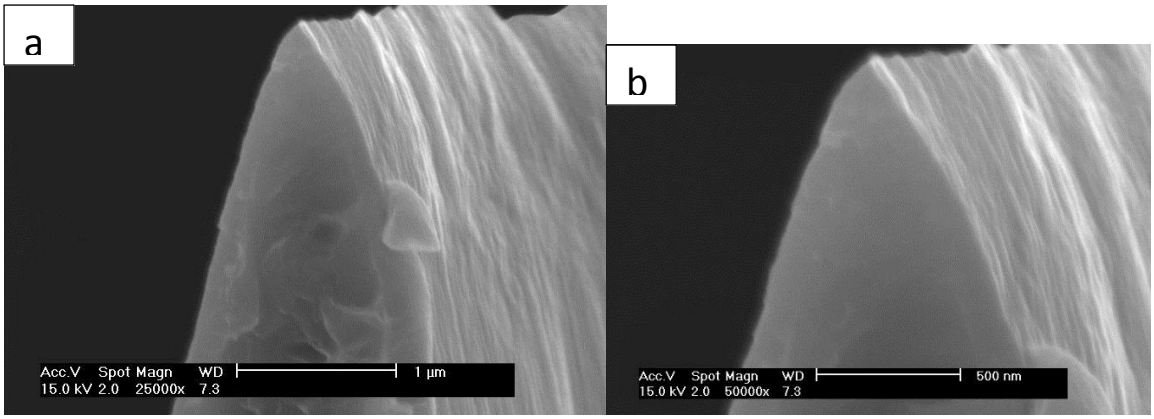

Figure 14. XSEM images of the tip of a razor blade coated with high irradiation C/Cr coating; a) low magnification image, b) high magnification image.

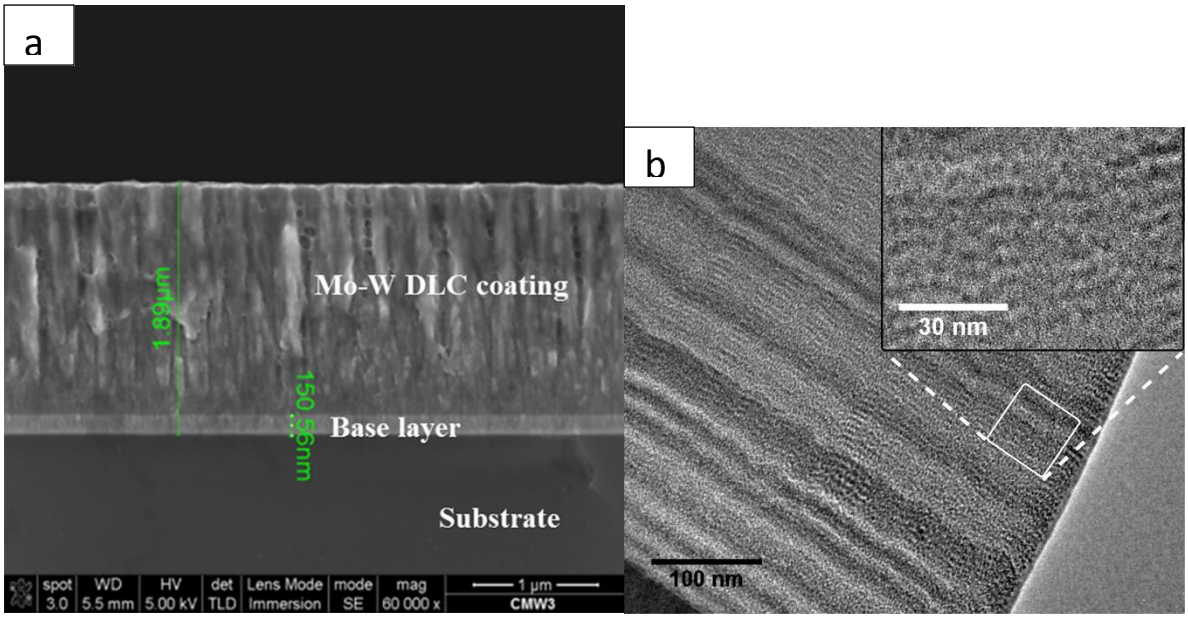

Figure 15: a) Cross-sectional SEM image, (reproduced from [65]), b) TEM image revealing the nanoscale multilayer structure of the Mo-W doped Carbon film, (reproduced from [66]).

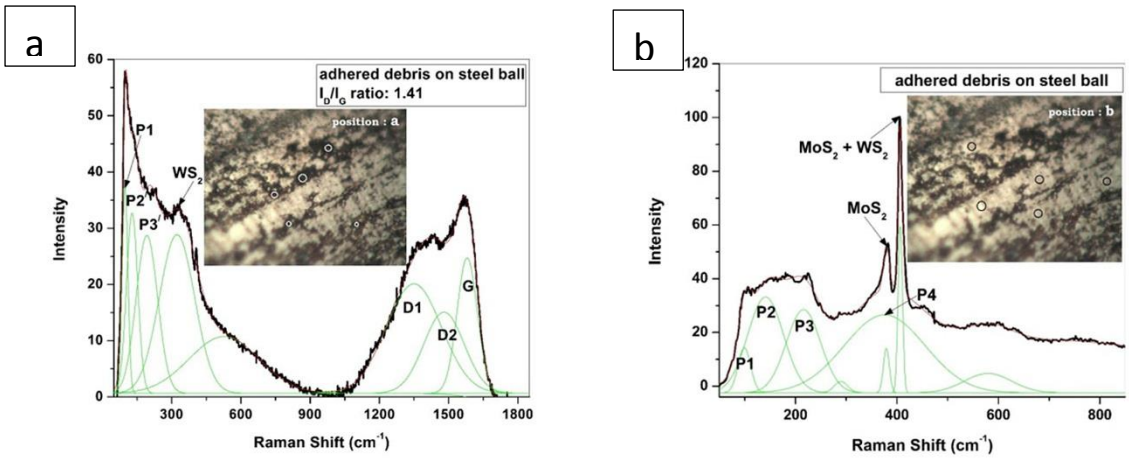

Figure 16 (a, b). Raman spectra collected from two types of wear debris adhered to the steel counterpart after sliding against Mo-W- doped C coating in a lubricated pin-on-disc test at 200 ^{o}C, (reproduced from [43]).

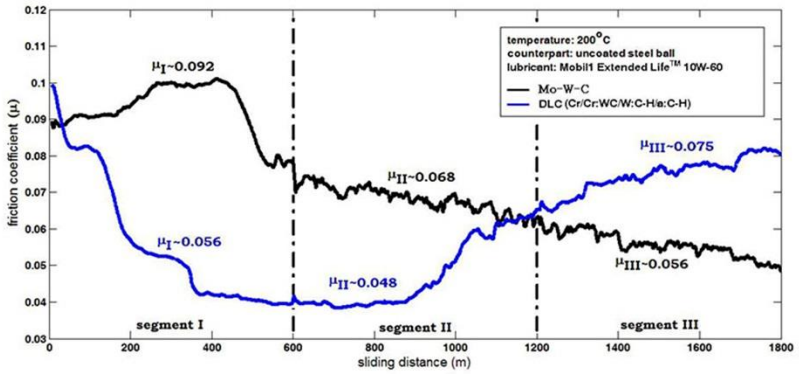

Figure 17. Friction behaviour of Mo-W- doped Carbon and hydrogenated DLC coating in lubricated sliding pin-on-disc test using 100Cr6 steel ball counterpart at 200°C, (reproduced from [65]).

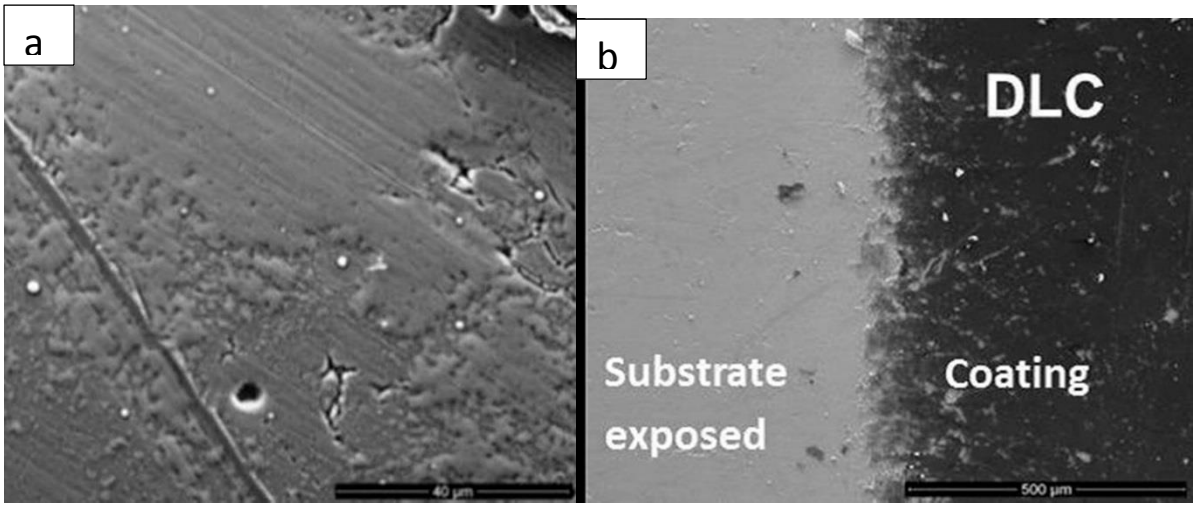

Figure18. SEM image of the surface after exposure to 500°C for 1 hour of: a) Mo-W-doped coating (reproduced from [67]) and b) DLC coating.

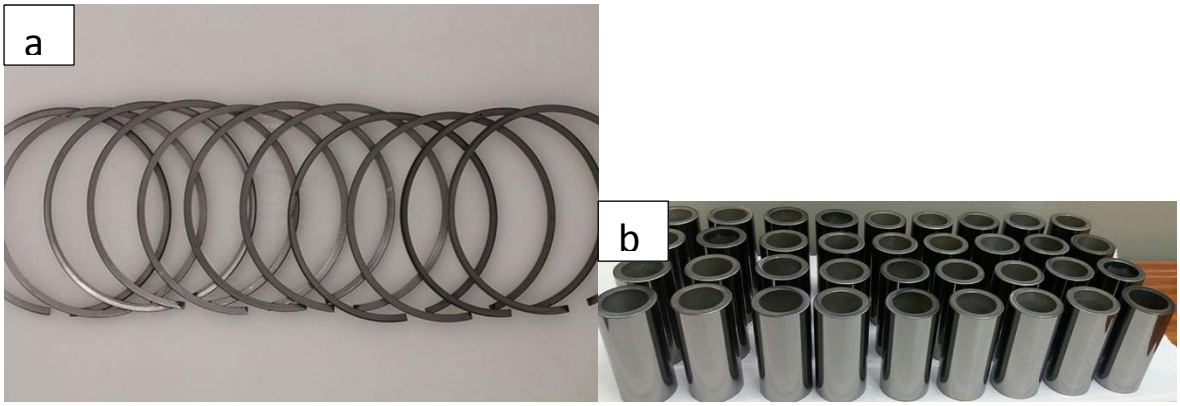

Figure 19. Mo-W- doped Carbon coated automotive components: a) piston rings, and b) tappets.

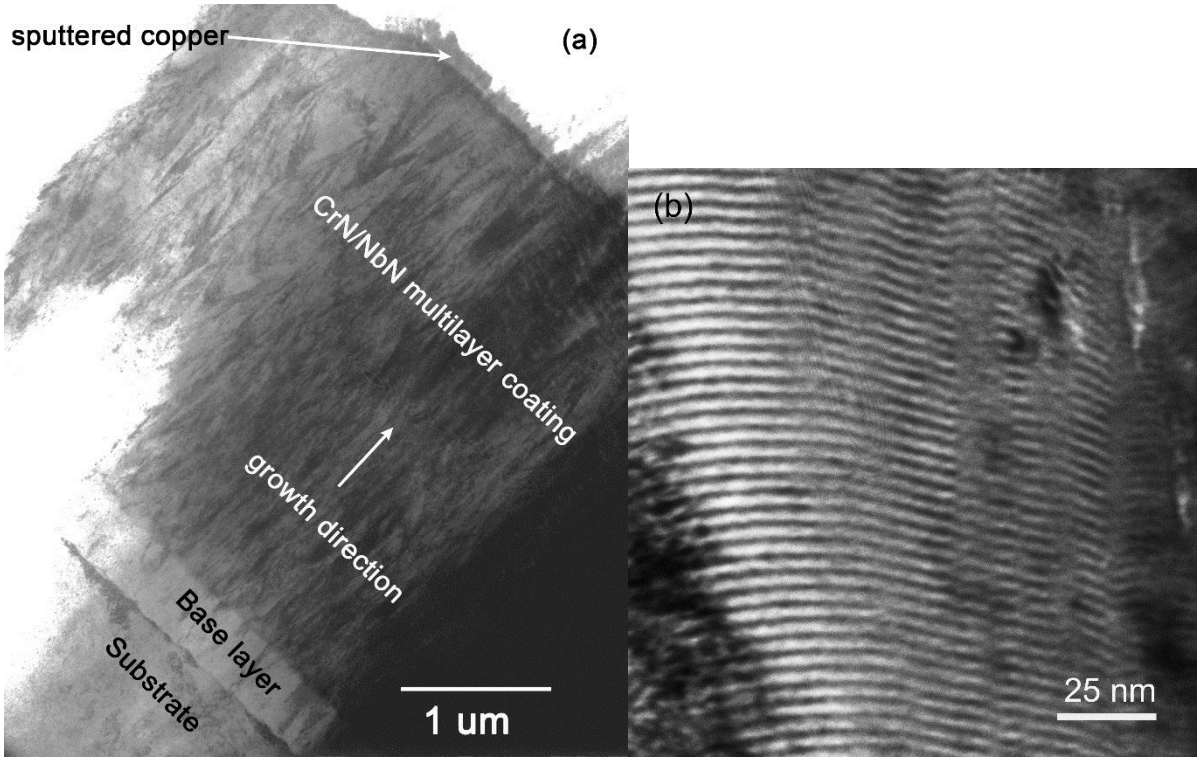

Figure 20. Bright field TEM (a) low magnification cross-section of the coating showing the overall CrN/NbN coating architecture and (b) high magnification image showing the multilayer structure on nanoscale, (reproduced from [78]).

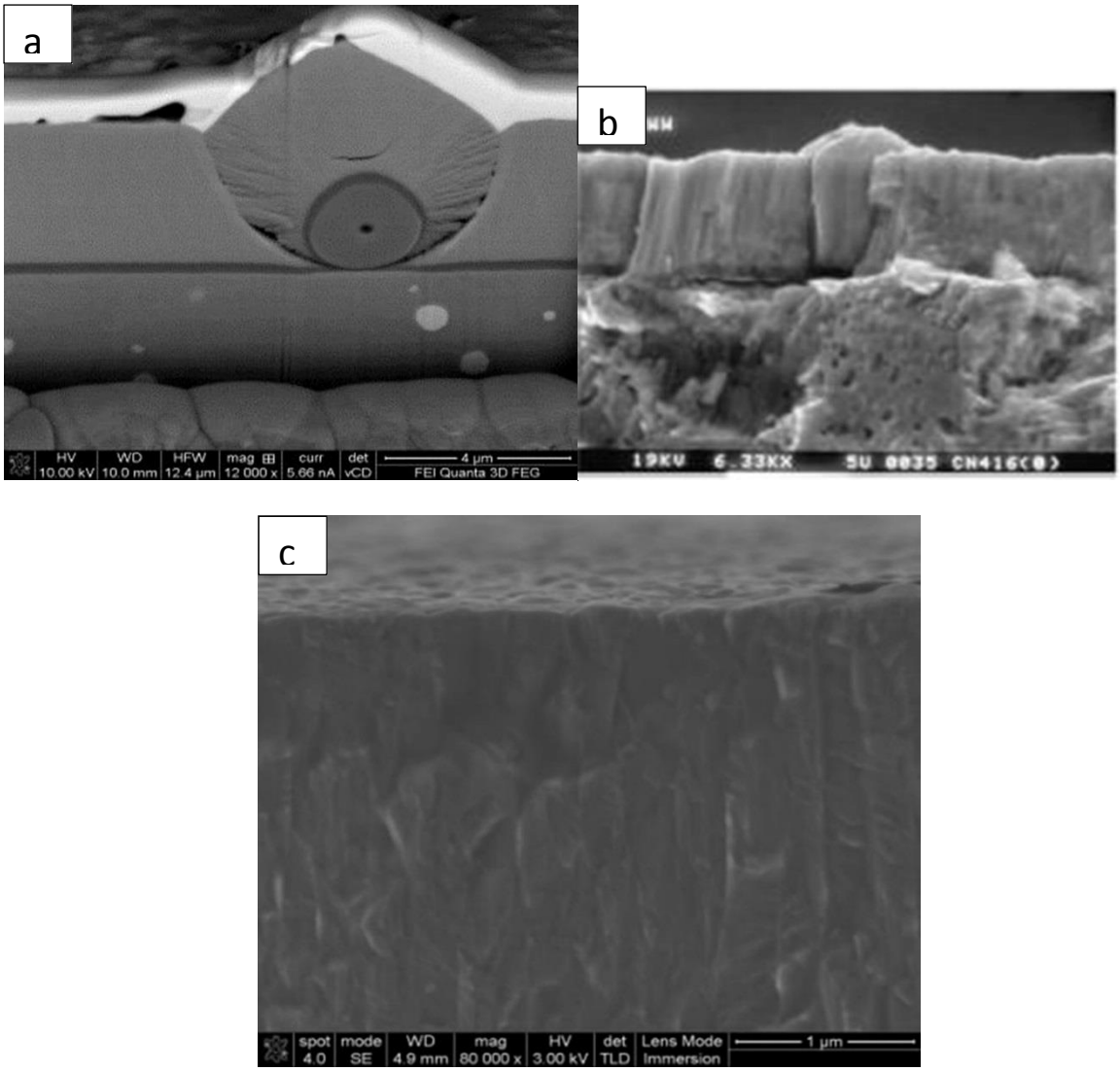

Figure 21: Cross sectional SEM images of CrN/NbN deposited by various techniques: a) Arc evaporation, (reproduced from [82]) b) Arc Bond Sputtering (ABS), c) HIPIMS,(reproduced from [82]).

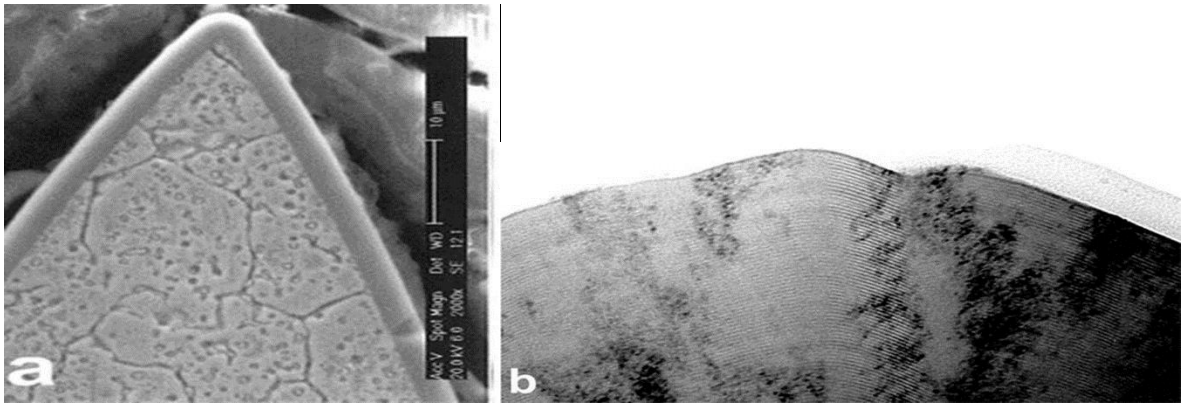

Figure 22: a) low magnification SEM, (reproduced from [77]) and b) XTEM images of CrN/NbN coating deposited on a scalpel blade, (reproduced from [11]).

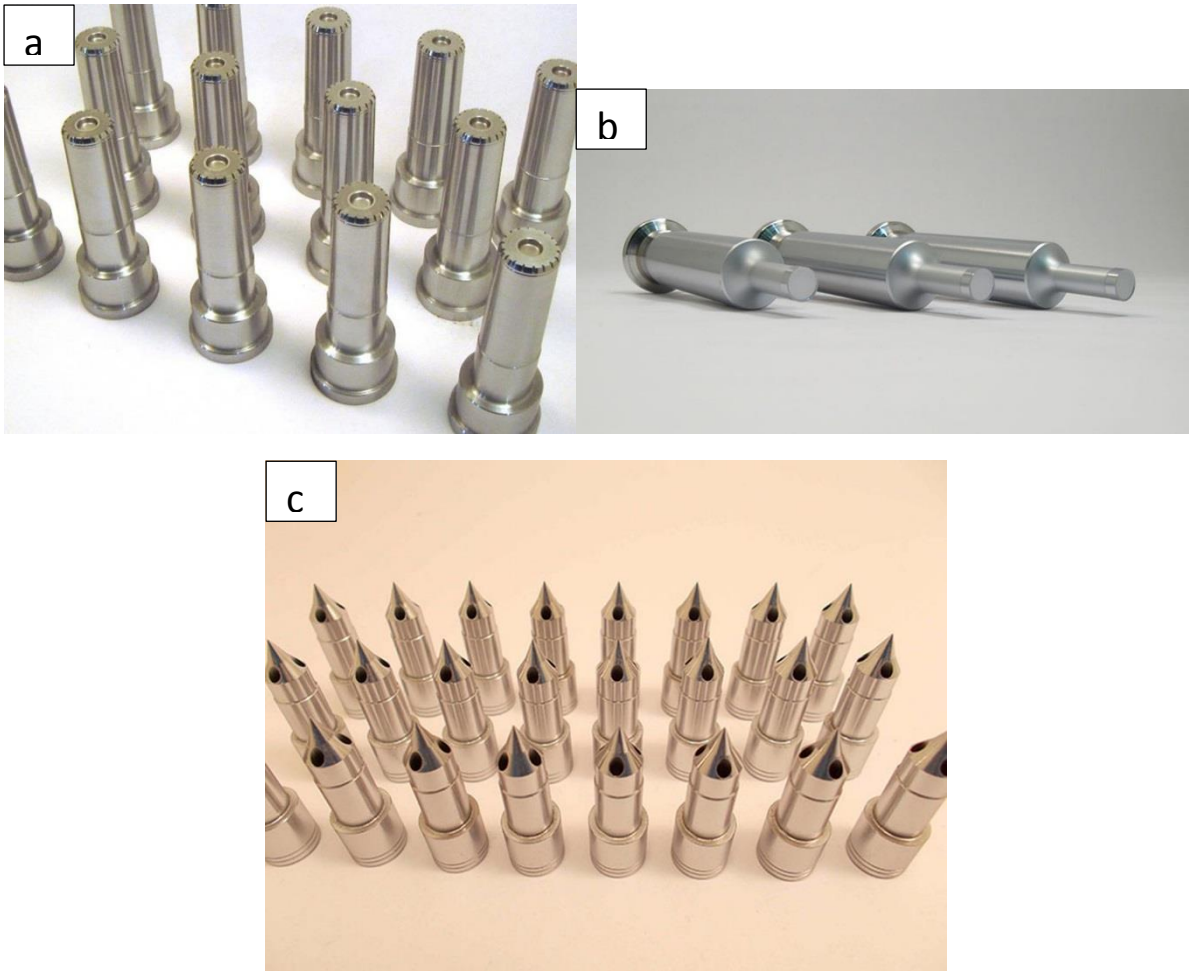

Figure 23. Various components coated with CrN/NbN at Lafer Spa, Italy: a) Plastic injection punches, b) Tablet pressing dies, c) Plastic injection heads. *Courtesy of Luidgi Parenti and Alessandro Bertè, Lafer Spa, Italy.*

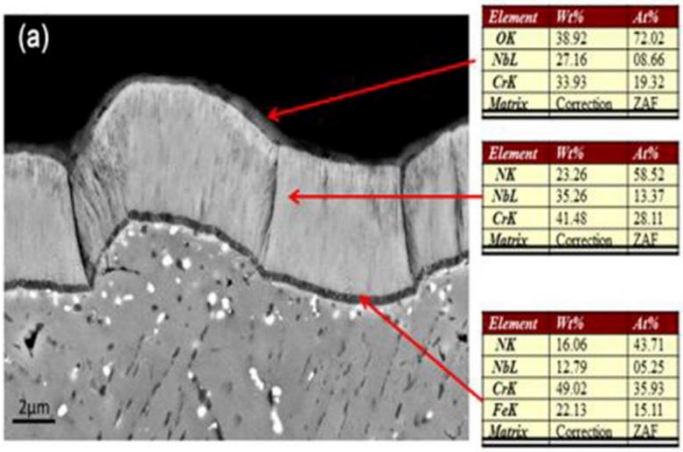

Figure 24. Cross sectional back scattered SEM image and EDX analysis data from localised regions of the CrN/NbN coating deposited on P92 steel after 2000 h exposure to 650°C in pure steam environment,(reproduced from [28]).

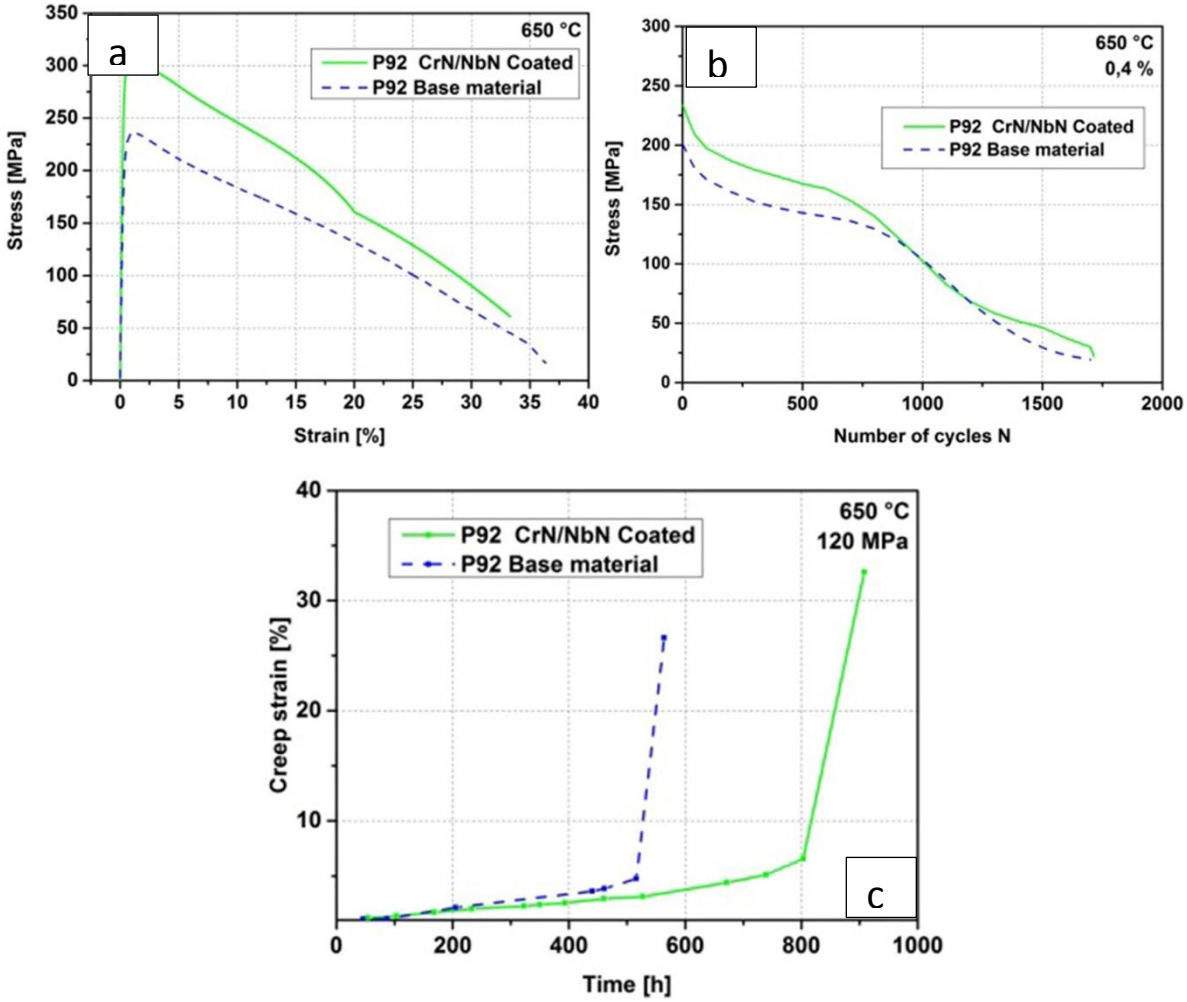

Figure 25. Mechanical tests of uncoated and coated P92 base material at 650°C: a) Stress-strain diagram, b) Cyclic stress response at constant strain amplitude of 0.4% and c) Creep curves of the coated and uncoated specimens tested at load of 120 MPa.

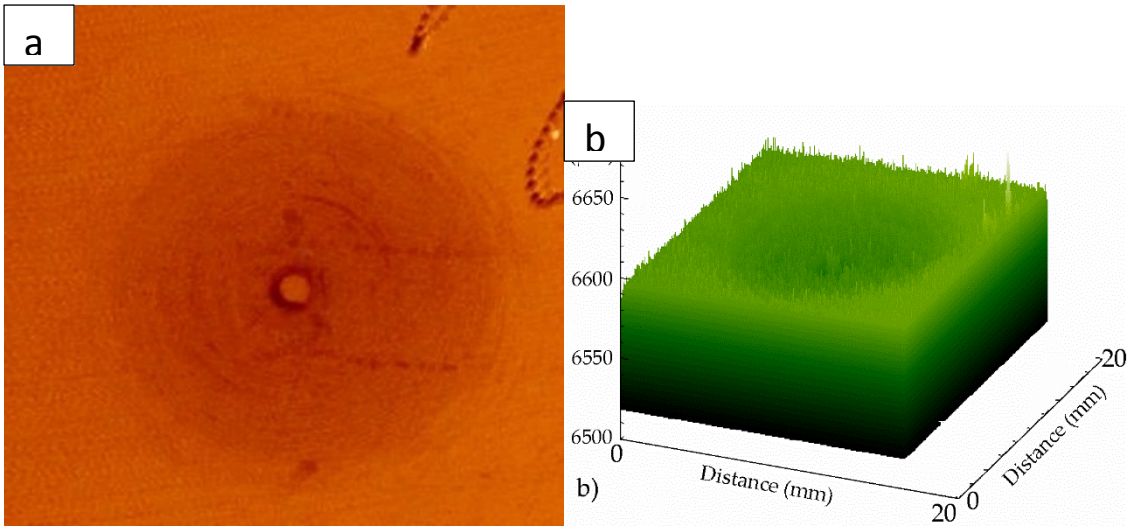

Figure 26. Droplet erosion test results: (a) 2-D Surface Plot (step size in x- and y-direction is 0.1 mm) (b) 3D Plot x- and y-steps 0.02 mm.

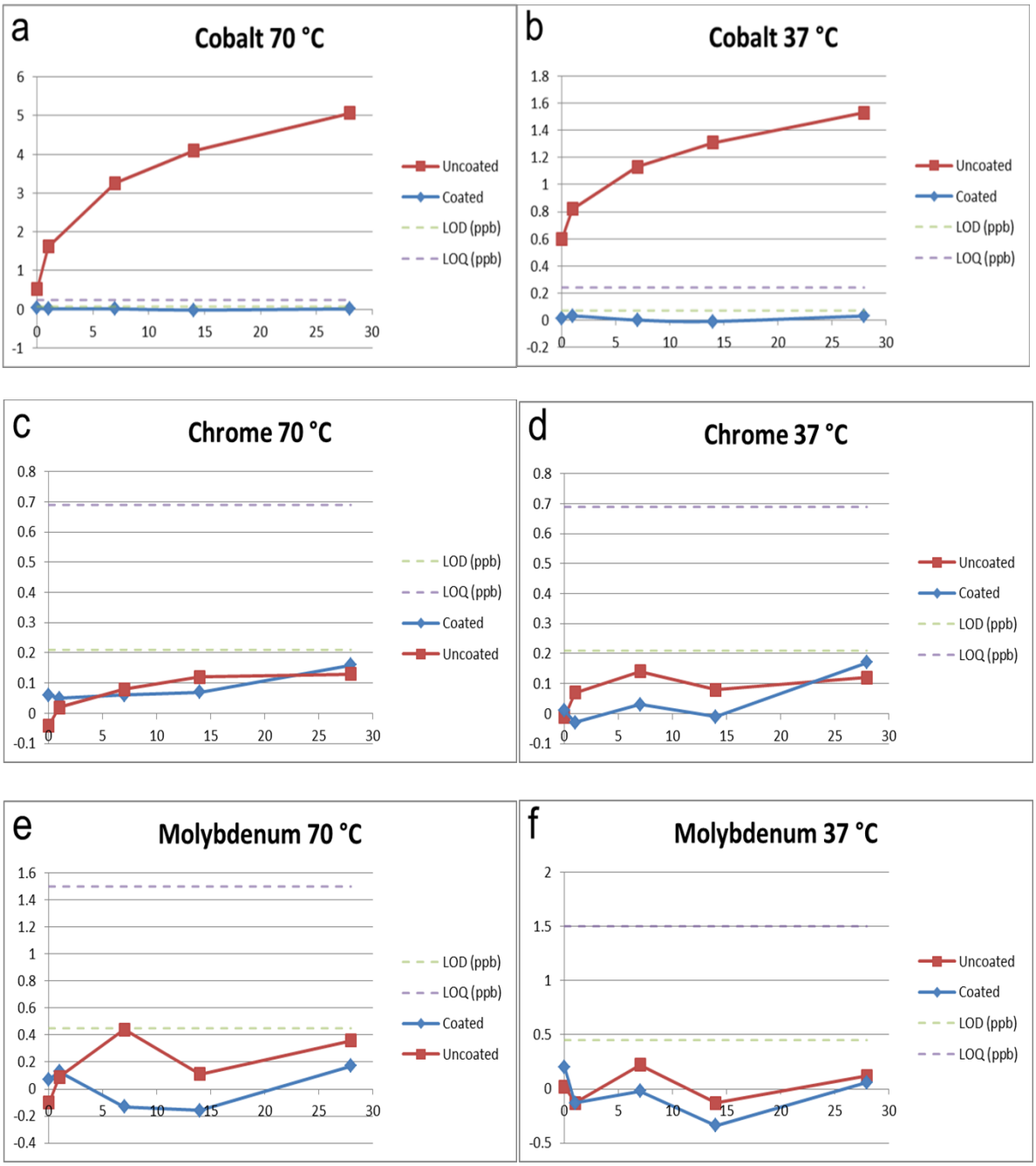

Figure 27. Ion release tests for Cr, Co and Mo at different time periods taken at high (70 °C) and low (37 °C) temperatures. LoD: limit of detection, LoQ: limit of quantification, (reproduced from [82].

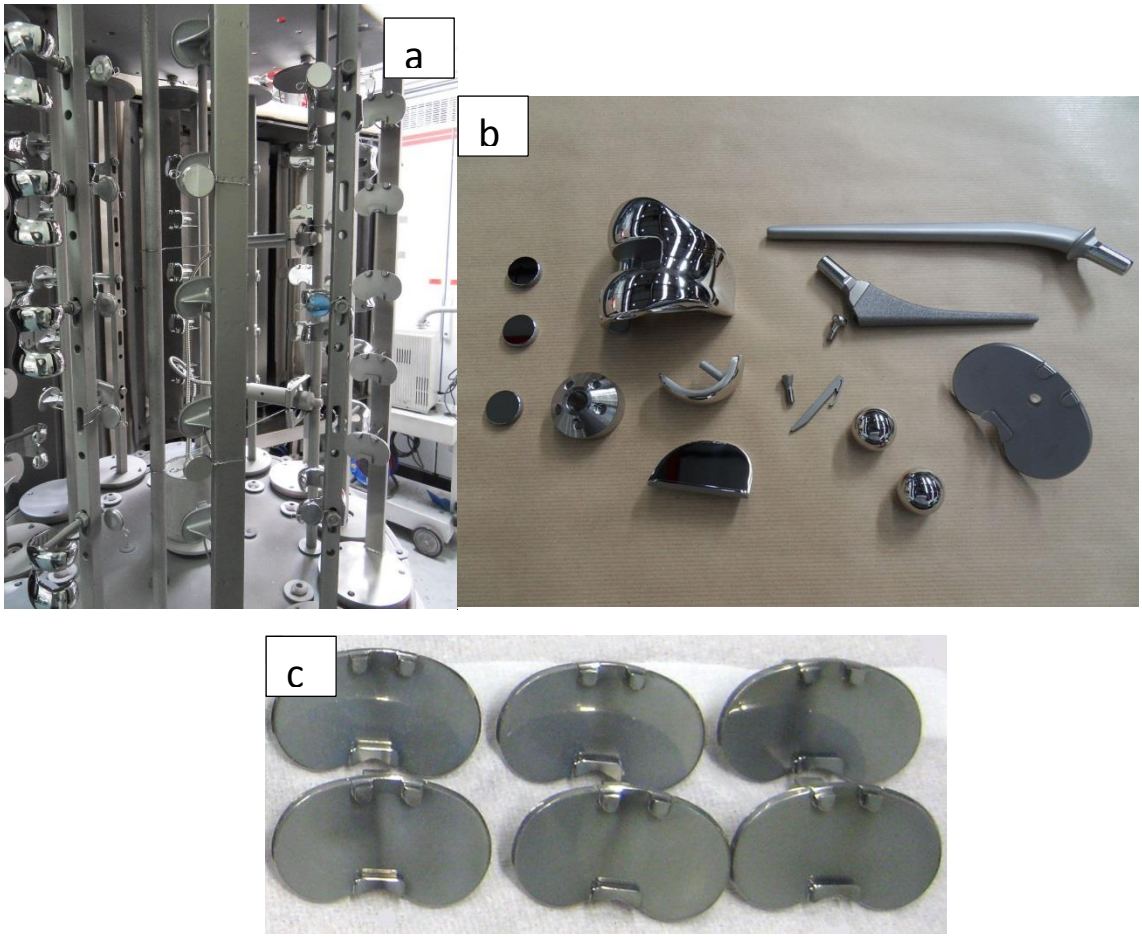

Figure 28. HIPIMS CrN/NbN coated knee implants at Ionbond UK: a) as loaded in the vacuum chamber and b) Femoral Heads, Tibial Plates and other implant components. *Courtesy of Dr. Chris Constable, Managing Director, Ionbond, UK, Ltd.*

Table 1. Properties of Hard Cr and CrN/NbN deposited by various techniques

Coating	Thickness (μm)	Hardness, HK 0.25N	Coefficient of Friction, μ	Wear Coefficient, Kc ($m^{-3}N^{-1}m^{1}$)	Corrosion Current Density, 3% NaCl (A. cm^{-2})
Electroplated Hard Cr	25	1400	0.72	5.8×10^{-14}	8.10^{-5}
CrN/NbN, ABS	4.0	3200	0.63	3.6×10^{-15}	$6.5.10^{-6}$
CrN/NbN, HIPIMS	4.0	3400	0.49	4.9×10^{-16}	$8.0.10^{-7}$